**Національна академія наук України**

**ІНСТИТУТ ФІЗИКИ КОНДЕНСОВАНИХ СИСТЕМ**

ICMP–05–05E

O. Derzhko, J. Richter, T. Krokhmalskii, O. Zaburannyi

THE GROUND–STATE AND THERMODYNAMIC PROPERTIES OF REGULARLY ALTERNATING SPIN–$\frac{1}{2}$ ANISOTROPIC $XY$ CHAINS

ЛЬВІВ

**УДК:** 538.9

**PACS:** 75.10.–b

**Властивості в основному стані і термодинамічні властивості регулярнозмінних спін–$\frac{1}{2}$ анізотропних $XY$ ланцюжків**

Олег Держко, Йоганес Ріхтер, Тарас Крохмальський, Олесь Забуранний

**Анотація.** Використовуючи перетворення Йордана–Вігнера і неперервні дроби, ми обчислюємо термодинамічні величини періодичного спін–$\frac{1}{2}$ поперечного ланцюжка Ізинга. Ми розглядаємо детально періоди модуляції 2 і 3. Ми порівнюємо термодинамічні властивості регулярнозмінних поперечних ланцюжків Ізинга і $XX$ ланцюжків; ми порівнюємо властивості в основному стані регулярнозміних квантових і класичних ланцюжків. Використовуючи унітарні перетворення, ми застосовуємо розроблений підхід до термодинаміки періодичних спін–$\frac{1}{2}$ анізотропних $XY$ ланцюжків без поля. Ми використовуємо енергію основного стану для періоду 2 щоб з'ясувати, як анізотропія обмінної взаємодії руйнує спін–пайєрлсову димеризацію.

**The ground–state and thermodynamic properties of regularly alternating spin–$\frac{1}{2}$ anisotropic $XY$ chains**

Oleg Derzhko, Johannes Richter, Taras Krokhmalskii, Oles' Zaburannyi

**Abstract.** Using the Jordan–Wigner transformation and continued fractions we calculate rigorously the thermodynamic quantities for the spin–$\frac{1}{2}$ transverse Ising chain with periodically varying intersite interactions or/and on–site fields. We consider in detail chains having periods of modulation 2 and 3. We compare the thermodynamic properties of regularly alternating transverse Ising and transverse $XX$ chains. Moreover, we compare the ground–state properties of regularly alternating quantum and classical chains. Making use of the corresponding unitary transformations we extend the elaborated approach for a study of thermodynamics of regularly alternating spin–$\frac{1}{2}$ anisotropic $XY$ chains without field. We use the exact expression for the ground–state energy of such a chain of period 2 to discuss how the exchange interaction anisotropy destroys the spin–Peierls dimerized phase.

## 1. Introductory remarks

The spin–$\frac{1}{2}$ Ising chain in a transverse field (transverse Ising chain) is known as the simplest model in the quantum theory of magnetism. It can be viewed as the 1D spin–$\frac{1}{2}$ anisotropic $XY$ model in a transverse ($z$) field with extremely anisotropic exchange interaction. By means of the Jordan–Wigner transformation it can be reduced to a 1D model of noninteracting spinless fermions [1–4]. As a result the transverse Ising chain appeared to be an easy case [5] and a lot of studies on that model have emerged up till now. After the properties of the basic skeleton model were understood various modifications were introduced into the model and the effects of the introduced changes were examined. For example, an analysis of the critical behaviour of the chain with an aperiodic sequence of interactions was performed in Ref. [6], an extensive real–space renormalization–group treatment of the random chain was reported in Ref. [7], a renormalization–group study of the aperiodic chain was presented in Ref. [8]. It should be remarked, however, that a simpler case of the *regularly inhomogeneous* spin–$\frac{1}{2}$ transverse Ising chain (in which the exchange interactions between nearest sites or/and the on–site transverse fields vary regularly along the chain with a finite period $p$) still contains enough not explored properties which deserve to be discussed. Moreover, the thermodynamic quantities of such a system can be derived *rigorously analytically* exploiting the fermionic representation and continued fractions.

The thermodynamic properties of the regularly alternating anisotropic $XY$ chain in a transverse field of period 2 were considered in Refs. [9, 10] (see also Ref. [11] where a model without field was investigated). The elaborated general approach for calculation of thermodynamic quantities [10] becomes rather tedious if $p > 2$ and the properties of chains of larger periods of alternation were not discussed. Other papers [12, 13] are devoted to the 1D anisotropic $XY$ model on superlattices, which can be viewed as particular cases of a regularly alternating anisotropic $XY$ chain. In Ref. [12] the transfer matrix method was applied to get the excitation spectrum of the Hamiltonian, being a quadratic form of creation and annihilation Bose or Fermi operators, on a 1D superlattice. (This fermionic system is related to the 1D spin–$\frac{1}{2}$ transverse anisotropic $XY$ model on a superlattice.) In Ref. [13] a version of the approach suggested in Ref. [10] was applied for superlattices. Considering as an example the ground–state dependences of the transverse magnetization vs. transverse field and of the static transverse susceptibility vs. transverse field (which were examined numerically for an anisotropic $XY$ chain of



period 4) the authors of Ref. [13] observed that they behave differently from the isotropic $XY$ model. Namely, the number of the critical fields at which the susceptibility becomes singular strongly depends on the concrete values of intersite interaction parameters in the case of anisotropic $XY$ model (contrary to the case of isotropic $XY$ model). The quantum critical points in the anisotropic $XY$ chains in a transverse field with periodically varying intersite interactions (having periods 2 and 3) were determined by the transfer matrix method in Ref. [14]. It was found that for periodic chains the number of quantum phase transition points may increase and its actual value depends not only on the period of modulation but also on the strengths of anisotropy and modulation of exchange interactions. Let also mention here a paper discussing the energy gap vanishing in the dimerized (i.e., period 2) anisotropic $XY$ chain without field [15] and a recent paper [16] which contains such an analysis for a nonzero transverse field.

In the present paper we shall consider a systematic method for the calculation of the thermodynamic quantities of the regularly alternating spin–$\frac{1}{2}$ transverse Ising chain which reproduces the known results and yields new ones. For this purpose we utilize an alternative approach not used in the references cited above. This approach is based on exploiting continued fractions [17] and seems to be a natural and convenient language for describing regularly alternating chains. Considering the chains of periods 2 and 3 we examine the generic effects induced by regular alternation. We discuss, in particular, the influence of regular alternation on the energy gap, the zero–temperature dependences of the transverse magnetization vs. transverse field and of the static transverse susceptibility vs. transverse field and on the temperature dependences of thermodynamic quantities. These rigorous analytical results completed by numerical calculations of the spin correlation functions demonstrate the effect of the regular alternation of Hamiltonian parameters on the quantum phase transition inherent in the spin–$\frac{1}{2}$ transverse Ising chain. We also compare the results for the transverse Ising chains with the corresponding ones for the isotropic $XY$ chains in a transverse field (transverse $XX$ chains). Moreover, we compare the ground–state properties of the quantum and classical regularly alternating transverse Ising/$XX$ chains.

The results obtained exploiting the continued fractions approach can be used to examine thermodynamics of the regularly alternating spin–$\frac{1}{2}$ anisotropic $XY$ chain without field since the latter model is related to a system of two spin–$\frac{1}{2}$ transverse Ising chains through certain unitary transformations. We use the exact expression for the ground–state energy

of the anisotropic $XY$ chain without field of period 2 to demonstrate the effects of anisotropy of exchange interaction on the spin–Peierls dimerization.

The outline of the paper is as follows. We begin with a description of the model and a discussion of some of its symmetry properties in Section 2. In Section 3 we explain how the continued fractions can be used to calculate exactly the Helmholtz free energy (and thus all thermodynamic quantities) of the regularly alternating transverse Ising chain having an arbitrary (finite) period of alternation of the Hamiltonian parameters. Further we present the results for chains of periods 2 and 3 examining the behaviour of the transverse magnetization, static transverse susceptibility, and spin correlation functions (Section 4) and of the specific heat (Section 5). We apply the elaborated continued fractions approach for examining the thermodynamic properties of the regularly alternating anisotropic $XY$ chain without field in Section 6. Some conclusions are given in Section 7.

## 2. The model. Unitary transformations

We consider $N \to \infty$ spins $\frac{1}{2}$ on a ring governed by the Hamiltonian

$$H = \sum_{n=1}^{N} \Omega_n s_n^z + \sum_{n=1}^{N} 2I_n s_n^x s_{n+1}^x, \qquad s_{N+1}^{\alpha} = s_1^{\alpha}. \tag{2.1}$$

Here $I_n$ is the (Ising) exchange interaction between the nearest sites $n$ and $n+1$ and $\Omega_n$ is the transverse field at the site $n$. We assume that these quantities vary regularly along the chain with period $p$, i.e., the sequence of parameters in (2.1) is $\Omega_1 I_1 \Omega_2 I_2 \ldots \Omega_p I_p \Omega_1 I_1 \Omega_2 I_2 \ldots \Omega_p I_p \ldots$ . Our goal is to examine the thermodynamic properties of the spin model (2.1).

Before starting to calculate the thermodynamic quantities of the introduced model let us extend the "duality" transformation to the inhomogeneous case. This transformation is long known for the uniform transverse Ising chain (see, for example, Refs. [3, 18]). For the Ising chain in a random transverse field such a transformation was discussed in Refs. [9, 19]. It can be easily proved that the partition function $Z = \mathrm{Tr} \exp(-\beta H)$ for two sequences of parameters $\ldots \Omega_n I_n \ldots$ and $\ldots I_{n-1} \Omega_n \ldots$ (or $\ldots I_n \Omega_{n+1} \ldots$ ) is the same. (It means that the fields and the interactions may be interchanged as $\Omega_n \to I_{n-1}$ and $I_n \to \Omega_n$ (or $\Omega_n \to I_n$ and $I_n \to \Omega_{n+1}$) remaining the partition function unchanged.)



Really, performing the unitary transformation

$$U = \prod_{p=1}^{N-1} \exp\left(\mathrm{i}\pi s_p^x s_{p+1}^y\right) \tag{2.2}$$

one finds that Eq. (2.1) transforms (with the accuracy to the not important for thermodynamics end terms) into

$$\begin{aligned} UHU^{+} &= \sum_{n=1}^{N} I_n s_{n+1}^z + \sum_{n=1}^{N} 2\Omega_n s_n^y s_{n+1}^y \\ &= \sum_{n=1}^{N} I_n s_n^z + \sum_{n=1}^{N} 2\Omega_{n+1} s_n^y s_{n+1}^y, \qquad s_{N+1}^{\alpha} = s_1^{\alpha} \end{aligned} \tag{2.3}$$

(to get the second equality we have renumbered the sites $n \to n-1$ that obviously does not change thermodynamics). As a result $R^z U H U^{+} R^{z+}$ with $R^z = \prod_{q=1}^{N} \exp\left(\mathrm{i}\frac{\pi}{2} s_q^z\right)$ (up to end effects) is again the transverse Ising chain, however, with the exchange interaction between the nearest sites $n$ and $n+1$ equals to $\Omega_n$ (or $\Omega_{n+1}$) and the transverse field at the site $n$ equals to $I_{n-1}$ (or $I_n$). Hence, such thermodynamic quantities as the Helmholtz free energy per site $f = -\frac{1}{N\beta} \ln Z$, the internal energy $e = f + \beta \frac{\partial f}{\partial \beta}$, the entropy $\frac{s}{k} = \beta^2 \frac{\partial f}{\partial \beta}$ or the specific heat $\frac{c}{k} = -\beta \frac{\partial}{\partial \beta} \frac{s}{k}$ (but not the transverse magnetization $m^z = \frac{\partial f}{\partial \Omega}$ or the static transverse susceptibility $\chi^z = \frac{\partial m^z}{\partial \Omega}$) of the models characterizing by the sequence of parameters $\Omega I \ldots$ and $I\Omega \ldots$ ($p = 1$), $\Omega_1 I_1 \Omega_2 I_2 \ldots$ and $I_2 \Omega_1 I_1 \Omega_2 \ldots$ (or $I_1 \Omega_2 I_2 \Omega_1 \ldots$ ) ($p = 2$), $\Omega_1 I_1 \Omega_2 I_2 \Omega_3 I_3 \ldots$ and $I_3 \Omega_1 I_1 \Omega_2 I_2 \Omega_3 \ldots$ (or $I_1 \Omega_2 I_2 \Omega_3 I_3 \Omega_1 \ldots$ ) ($p = 3$) etc. are the same.

Let us also recall that the unitary transformation $F_m = 2s_m^x$ changes the sign of the transverse field at site $m$ in the Hamiltonian (2.1), whereas the unitary transformation $B_m = (2s_1^z) \ldots (2s_m^z)$ changes the sign of the exchange interaction between the sites $m$ and $m+1$ in the Hamiltonian (2.1). Therefore, in what follows we may assume without a loss of generality all exchange interactions to be positive $I_n \geq 0$. Although the thermodynamic quantities do not depend on the signs of the transverse fields $\Omega_n$ we do not impose a similar restriction for the signs of the fields since we shall also discuss the behaviour of such quantities as the transverse magnetization and the static transverse susceptibility which arise after differentiation with respect to the transverse field. The symmetry remarks permit to reduce the range of parameters for the study of the thermodynamics of the model.

Finally, let us extend to the inhomogeneous case the relation between the anisotropic $XY$ chain without field and the transverse Ising chain (see, for example, Refs. [19, 20]). Applying to the Hamiltonian

$$H = \sum_{n=1}^{N} \left(2I_n^x s_n^x s_{n+1}^x + 2I_n^y s_n^y s_{n+1}^y\right), \qquad (2.4)$$
$$s_{N+1}^\alpha = s_1^\alpha$$

the unitary transformation

$$V = \prod_{p=1}^{N-1} \exp\left(\mathrm{i}\pi s_p^y s_{p+1}^z\right) \qquad (2.5)$$

one gets with an accuracy to end terms

$$VHV^+ = \sum_{n=1}^{N} \left(2I_n^x s_n^z s_{n+2}^z + I_n^y s_{n+1}^x\right), \qquad (2.6)$$
$$s_{N+1}^\alpha = s_1^\alpha.$$

This is the Hamiltonian of two independent chains. Performing further a $\frac{\pi}{2}$ rotation of all spins about $y$–axis one finds that $R^y V H V^+ R^{y+}$, $R^y = \prod_{q=1}^{N} \exp\left(\mathrm{i}\frac{\pi}{2} s_q^y\right)$ (up to end effects) is the Hamiltonian of two independent transverse Ising chains (in the notations used in Eq. (2.1)) each of $\frac{N}{2}$ sites defined by the sequences of parameters $\ldots I_{n+1}^y I_{n+2}^x I_{n+3}^y I_{n+4}^x \ldots$ and $\ldots I_n^y I_{n+1}^x I_{n+2}^y I_{n+3}^x \ldots$ . If the chain (2.4) is isotropic, i.e., $I_n^x = I_n^y = I_n$, the two transverse Ising chains have the same thermodynamics. Thus, the $XX$ chain of $N$ sites without field defined by a sequence of parameters $\ldots I_n I_{n+1} \ldots$ is thermodynamically equivalent to two identical transverse Ising chains of $\frac{N}{2}$ sites with the sequence of parameters $\ldots I_n I_{n+1} \ldots$ . We shall use the discussed relation in Section 6 to study the thermodynamic properties of regularly alternating anisotropic $XY$ chains without field.

## 3. Continued fraction approach

### 3.1. The density of states and thermodynamic quantities

To derive the thermodynamic quantities of the spin model (2.1) we first express the spin Hamiltonian in fermionic language by applying the



Jordan–Wigner transformation [1–5]. As a result we arrive at a model of spinless fermions on a ring governed by the Hamiltonian

$$H = \sum_{n=1}^{N} \Omega_n \left(c_n^+ c_n - \frac{1}{2}\right)$$
$$+\frac{1}{2}\sum_{n=1}^{N} I_n \left(c_n^+ c_{n+1}^+ + c_n^+ c_{n+1} - c_n c_{n+1}^+ - c_n c_{n+1}\right), \qquad (3.1)$$
$$c_{N+1}^+ = c_1^+, \quad c_{N+1} = c_1$$

(the boundary term, that is unimportant as far as the thermodynamics is concerned, has been omitted). It is well known [1, 3, 19, 21] that the Hamiltonian (3.1) can be transformed into the diagonal form

$$H = \sum_{k=1}^{N} \Lambda_k \left(\eta_k^+ \eta_k - \frac{1}{2}\right), \qquad (3.2)$$
$$\left\{\eta_k^+, \eta_q\right\} = \delta_{kq}, \quad \left\{\eta_k, \eta_q\right\} = \left\{\eta_k^+, \eta_q^+\right\} = 0$$

after introducing new operators

$$\eta_k = \sum_{i=1}^{N} \left(g_{ki} c_i + h_{ki} c_i^+\right), \quad \eta_k^+ = \sum_{i=1}^{N} \left(h_{ki} c_i + g_{ki} c_i^+\right) \qquad (3.3)$$

where the coefficients

$$g_{ki} = \frac{1}{2}(\Phi_{ki} + \Psi_{ki}), \quad h_{ki} = \frac{1}{2}(\Phi_{ki} - \Psi_{ki}) \qquad (3.4)$$

are determined from the following equations

$$\Omega_{n-1} I_{n-1} \Phi_{k,n-1} + \left(\Omega_n^2 + I_{n-1}^2 - \Lambda_k^2\right) \Phi_{kn} + \Omega_n I_n \Phi_{k,n+1} = 0, \qquad (3.5)$$
$$\Phi_{k0} = \Phi_{kN}, \quad \Phi_{k,N+1} = \Phi_{k1};$$

$$\Omega_n I_{n-1} \Psi_{k,n-1} + \left(\Omega_n^2 + I_n^2 - \Lambda_k^2\right) \Psi_{kn} + \Omega_{n+1} I_n \Psi_{k,n+1} = 0, \qquad (3.6)$$
$$\Psi_{k0} = \Psi_{kN}, \quad \Psi_{k,N+1} = \Psi_{k1}.$$

Evidently, we may obtain the thermodynamic quantities of the spin model (2.1) having the density of states

$$R(E^2) = \frac{1}{N} \sum_{k=1}^{N} \delta(E^2 - \Lambda_k^2) \qquad (3.7)$$

since due to Eq. (3.2) the Helmholtz free energy per site is given by

$$f = -\frac{2}{\beta}\int_0^\infty \mathrm{d}EER(E^2)\ln\left(2\cosh\frac{\beta E}{2}\right). \tag{3.8}$$

(As we shall see below the density of states $R(E^2)$ (which contains the same information as a set of all $\Lambda_k$) is easier to calculate than the values of $\Lambda_k$ or the coefficients $g_{ki}$, $h_{ki}$.)

On the other hand, we may exploit Eqs. (3.5), (3.6) to obtain the desired density of states $R(E^2)$ (3.7). We note that a three diagonal band set of equations (3.5) (or (3.6)) strongly resembles the one describing displacements of particles in a nonuniform harmonic chain with nearest neighbour interactions and $R(E^2)$ (3.7) plays a role of the distribution of the squared phonon frequencies (for a study of the phonon density of states in a linear nonuniform system see, for example, Ref. [22]). The set of equations (3.5) (or (3.6)) can be also viewed as the one for determining a wave function of (spinless) electron in the 1D nonuniform tight–binding model.

To find the density of states $R(E^2)$ from the set of equations (3.5) (or (3.6)) we use the standard Green function approach. Consider, for example, Eq. (3.5). Let us introduce the Green functions $G_{nm} = G_{nm}(E^2)$ which satisfy the set of equations

$$\left(E^2 - \Omega_n^2 - I_{n-1}^2\right)G_{nm} - \Omega_{n-1}I_{n-1}G_{n-1,m} - \Omega_n I_n G_{n+1,m} = \delta_{nm} \tag{3.9}$$

with periodic boundary conditions implied. Knowing the diagonal Green functions $G_{nn} = G_{nn}(E^2)$ we immediately find the density of states $R(E^2)$ (3.7) through the relation

$$R(E^2) = \mp\frac{1}{\pi N}\sum_{n=1}^{N}\mathrm{Im}G_{nn}(E^2 \pm \mathrm{i}\epsilon), \quad \epsilon \to +0. \tag{3.10}$$

Alternatively, $R(E^2)$ can be obtained with the help of the Green functions introduced on the basis of the set of equations for coefficients $\Psi_{kn}$ (3.6). The set of equations for such Green functions (like Eq. (3.9)) corresponds to the unitary equivalent spin chain (see (2.2), (2.3)) which exhibits the same thermodynamic properties. Thus, the resulting density of states $R(E^2)$ is the same.

We have now to calculate the diagonal Green functions $G_{nn}$ involved into Eq. (3.10). Let us use the continued fraction representation for $G_{nn}$



that follows from (3.9)

$$G_{nn} = \frac{1}{E^2 - \Omega_n^2 - I_{n-1}^2 - \Delta_n^- - \Delta_n^+}, \tag{3.11}$$

$$\Delta_n^- = \cfrac{\Omega_{n-1}^2 I_{n-1}^2}{E^2 - \Omega_{n-1}^2 - I_{n-2}^2 - \cfrac{\Omega_{n-2}^2 I_{n-2}^2}{E^2 - \Omega_{n-2}^2 - I_{n-3}^2 - \ddots}},$$

$$\Delta_n^+ = \cfrac{\Omega_n^2 I_n^2}{E^2 - \Omega_{n+1}^2 - I_n^2 - \cfrac{\Omega_{n+1}^2 I_{n+1}^2}{E^2 - \Omega_{n+2}^2 - I_{n+1}^2 - \ddots}}.$$

(Note that the signs of exchange interactions and fields are not important for the thermodynamic quantities as was noted above and is explicitly seen from Eq. (3.11).) For any finite period of varying $\Omega_n$ and $I_n$ the continued fractions in (3.11) become periodic (in the limit $N \to \infty$) and can be easily calculated by solving quadratic equations. As a result we get rigorous expressions for the Green functions, density of states (3.10) and thermodynamic quantities of the periodically alternating spin chain (2.1). For example, the entropy and specific heat are given by

$$\frac{s}{k} = 2\int_0^\infty \mathrm{d}EER(E^2)\left(\ln\left(2\cosh\frac{\beta E}{2}\right) - \frac{\beta E}{2}\tanh\frac{\beta E}{2}\right) \tag{3.12}$$

and

$$\frac{c}{k} = 2\int_0^\infty \mathrm{d}EER(E^2)\left(\frac{\frac{\beta E}{2}}{\cosh\frac{\beta E}{2}}\right)^2, \tag{3.13}$$

respectively. Assuming that $\Omega_n = \Omega + \Delta\Omega_n$ one can also obtain the transverse magnetization

$$m^z = \frac{\partial f}{\partial \Omega} = -\frac{2}{\beta}\int_0^\infty \mathrm{d}EE\frac{\partial R(E^2)}{\partial \Omega}\ln\left(2\cosh\frac{\beta E}{2}\right) \tag{3.14}$$

and the static transverse susceptibility

$$\chi^z = \frac{\partial m^z}{\partial \Omega} = -\frac{2}{\beta}\int_0^\infty \mathrm{d}EE\frac{\partial^2 R(E^2)}{\partial \Omega^2}\ln\left(2\cosh\frac{\beta E}{2}\right). \tag{3.15}$$

Following the procedure described above, for the periodically alter-

nating chain of period 2 we find the following result for $R(E^2)$

$$R(E^2) = \begin{cases} \frac{1}{2\pi}\frac{|\mathcal{Y}(E^2)|}{\sqrt{\mathcal{B}(E^2)}}, & \text{if} \quad \mathcal{B}(E^2) > 0, \\ 0, & \text{otherwise}, \end{cases} \tag{3.16}$$

$$\mathcal{Y}(E^2) = 2E^2 - \Omega_1^2 - \Omega_2^2 - I_1^2 - I_2^2,$$

$$\mathcal{B}(E^2) = 4\Omega_1^2\Omega_2^2 I_1^2 I_2^2 - \left(E^4 - \left(\Omega_1^2 + \Omega_2^2 + I_1^2 + I_2^2\right) E^2 + \Omega_1^2\Omega_2^2 + I_1^2 I_2^2\right)^2$$
$$= -(E^2 - b_1)(E^2 - b_2)(E^2 - b_3)(E^2 - b_4),$$

$$\{b_j\} = \left\{ \frac{1}{2}\left(\Omega_1^2 + \Omega_2^2 + I_1^2 + I_2^2 \pm \sqrt{(\Omega_1^2 + \Omega_2^2 + I_1^2 + I_2^2)^2 - 4(\Omega_1\Omega_2 \pm I_1 I_2)^2}\right)\right\}.$$

For the periodically alternating chain of period 3 we find

$$R(E^2) = \begin{cases} \frac{1}{3\pi}\frac{|\mathcal{X}(E^2)|}{\sqrt{\mathcal{C}(E^2)}}, & \text{if} \quad \mathcal{C}(E^2) > 0, \\ 0, & \text{otherwise}, \end{cases} \tag{3.17}$$

$$\mathcal{X}(E^2) = 3E^4 - 2\left(\Omega_1^2 + \Omega_2^2 + \Omega_3^2 + I_1^2 + I_2^2 + I_3^2\right) E^2 + \Omega_1^2\Omega_2^2 + \Omega_1^2 I_2^2 + I_1^2 I_2^2 + \Omega_2^2\Omega_3^2 + \Omega_2^2 I_3^2 + I_2^2 I_3^2 + \Omega_3^2\Omega_1^2 + \Omega_3^2 I_1^2 + I_3^2 I_1^2,$$

$$\mathcal{C}(E^2) = 4\Omega_1^2\Omega_2^2\Omega_3^2 I_1^2 I_2^2 I_3^2 - \left(E^6 - \left(\Omega_1^2 + \Omega_2^2 + \Omega_3^2 + I_1^2 + I_2^2 + I_3^2\right) E^4 + \left(\Omega_1^2\Omega_2^2 + \Omega_1^2 I_2^2 + I_1^2 I_2^2 + \Omega_2^2\Omega_3^2 + \Omega_2^2 I_3^2 + I_2^2 I_3^2 + \Omega_3^2\Omega_1^2 + \Omega_3^2 I_1^2 + I_3^2 I_1^2\right) E^2 - \Omega_1^2\Omega_2^2\Omega_3^2 - I_1^2 I_2^2 I_3^2\right)^2$$
$$= -(E^2 - c_1)(E^2 - c_2)(E^2 - c_3)(E^2 - c_4)(E^2 - c_5)(E^2 - c_6),$$

where $c_1, \ldots, c_6$ are the roots of two qubic equations which follow from the equation $\mathcal{C}(E^2) = 0$ (3.17).

Eqs. (3.16), (3.17) recover the result for the uniform chain if $\Omega_n = \Omega$, $I_n = I$ as it should be. The obtained density of states for $p = 2$ (3.16) can be compared with the exact calculation for the anisotropic $XY$ chain in a transverse field reported in Ref. [10]. Such a spin chain is represented



by noninteracting spinless fermions with the Hamiltonian

$$H = \sum_{-\frac{\pi}{2} < k < \frac{\pi}{2}} \sum_{\nu = \pm} \Lambda_{k\nu} \left(\eta_{k\nu}^+ \eta_{k\nu} - \frac{1}{2}\right), \tag{3.18}$$

$$\Lambda_{k\pm}^2 = \Omega_+^2 + \Omega_-^2 + \left(I_{+++}^2 + I_{--+}^2\right)\cos^2 k + \left(I_{-+-}^2 + I_{+--}^2\right)\sin^2 k \pm 2\left(\Omega_+^2\Omega_-^2 + \left(I_{+++}I_{---}\cos^2 k + I_{-+-}I_{+--}\sin^2 k\right)^2 + \left(\Omega_+^2 I_{+++}^2 + \Omega_-^2 I_{--+}^2\right)\cos^2 k + \left(\Omega_+^2 I_{-+-}^2 + \Omega_-^2 I_{+--}^2\right)\sin^2 k\right)^{\frac{1}{2}},$$

$$I_{\pm\pm\pm} = \frac{1}{2}\left(I_1^x \pm I_2^x \pm I_1^y \pm I_2^y\right), \quad \Omega_\pm = \frac{1}{2}\left(\Omega_1 \pm \Omega_2\right),$$

$$\left\{\eta_{k'\nu'}^+, \eta_{k''\nu''}\right\} = \delta_{k'k''}\delta_{\nu'\nu''}, \quad \left\{\eta_{k'\nu'}, \eta_{k''\nu''}\right\} = \left\{\eta_{k'\nu'}^+, \eta_{k''\nu''}^+\right\} = 0.$$

Therefore, the density of states (3.7) for the transverse Ising chain of period 2 which follows from Eq. (3.18) has the form

$$R(E^2) = \frac{1}{2\pi}\int_{-\frac{\pi}{2}}^{\frac{\pi}{2}} \mathrm{d}k\,\delta\left(E^2 - \Lambda_{k+}^2\right) + \frac{1}{2\pi}\int_{-\frac{\pi}{2}}^{\frac{\pi}{2}} \mathrm{d}k\,\delta\left(E^2 - \Lambda_{k-}^2\right), \tag{3.19}$$

$$\Lambda_{k\pm}^2 = \frac{1}{2}\left(\Omega_1^2 + \Omega_2^2 + I_1^2 + I_2^2\right) \pm \sqrt{\frac{1}{4}\left(\Omega_1^2 + \Omega_2^2 + I_1^2 + I_2^2\right)^2 - \Omega_1^2\Omega_2^2 - I_1^2 I_2^2 + 2\Omega_1\Omega_2 I_1 I_2 \cos(2k)}$$

and after integration transforms into (3.16).

### 3.2. The energy gap and quantum phase transition points

The density of states $R(E^2)$ (3.7) yields valuable information about the spectral properties of the Hamiltonian (2.1). Thus, the gap $\Delta$ in the energy spectrum of the spin chain is given by the square root of the smallest root of the polynomial $\mathcal{B}(E^2)$ if $p = 2$, $\mathcal{C}(E^2)$ if $p = 3$ etc.. In Figs. 1, 2 and Fig. 3 we display the dependence of the energy gap on the transverse field[1] for chains of period 2 and period 3, respectively. In Fig. 2 we also show this dependence for a chain of period 2 with anisotropic exchange interaction ($2I_n s_n^x s_{n+1}^x \to 2I_n\left((1+\gamma)s_n^x s_{n+1}^x + (1-\gamma)s_n^y s_{n+1}^y\right)$ in (2.1))

[1] Hereafter we fix $\Delta\Omega_n$ ($\Omega_n = \Omega + \Delta\Omega_n$, $\sum_n \Delta\Omega_n = 0$) and $I_n$ and assume $\Omega$ to be a free parameter. As a result we consider the changes in different properties as the transverse field (and temperature) varies. Obviously, while fixing $\Omega_n$ and $\Delta I_n$ ($I_n = I + \Delta I_n$, $\sum_n \Delta I_n = 0$) and assuming $I$ to be a free parameter (in such a case, e.g., the quantum phase transition is driven by tuning the exchange interaction $I$ rather than the transverse field $\Omega$) we recover the "violated" symmetry between transverse field and exchange interaction.

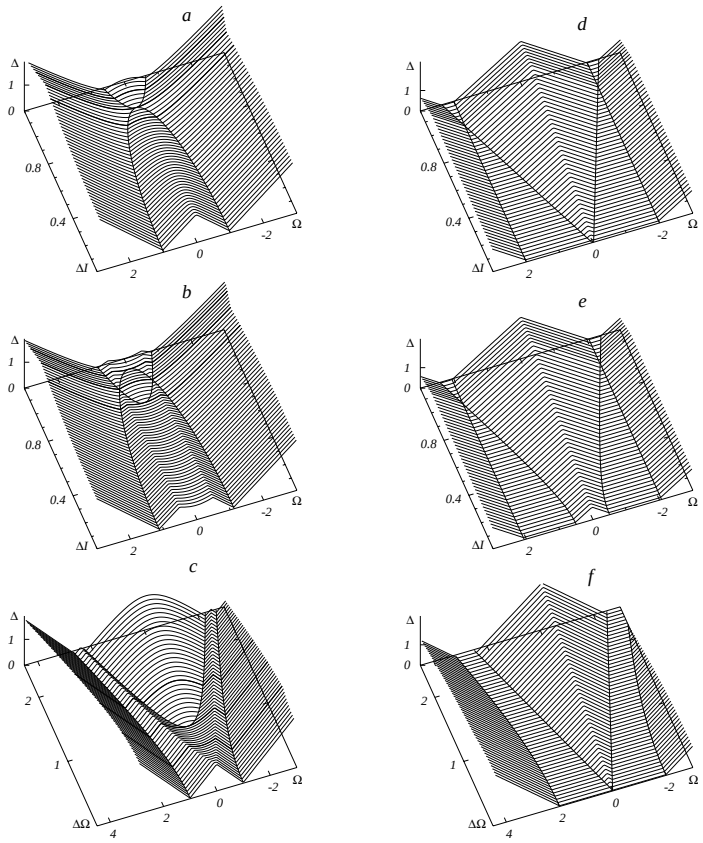


Figure 1. The energy gap $\Delta$ vs. transverse field $\Omega$ for spin–$\frac{1}{2}$ $XY$ chains of period 2 (a – c: transverse Ising chains, d – f: transverse $XX$ chains; $\Omega_{1,2} = \Omega \pm \Delta\Omega$, $I_{1,2} = 1 \pm \Delta I$; $\Delta\Omega = 0$ (a, d); $\Delta\Omega = 0.5$ (b, e); $\Delta I = 0$ (c, f)). The bold curves $\Delta$ vs. $\Omega$ correspond to the following values of parameters: $\Delta I = 0.9,\ 1,\ 1.1$ (panel a), $\Delta I = \sqrt{0.75} \approx 0.866,\ 1,\ \sqrt{1.25} \approx 1.118$ (panel b), $\Delta\Omega = 0.5,\ 1,\ 1.5$ (panel c). The bold curves in the planes $\Omega$–$\Delta I$ and $\Omega$–$\Delta\Omega$ indicate the values of parameters of transverse Ising chains (the boundaries of the region of parameters of transverse $XX$ chains) which yield the zero–energy gap, $\Delta = 0$.



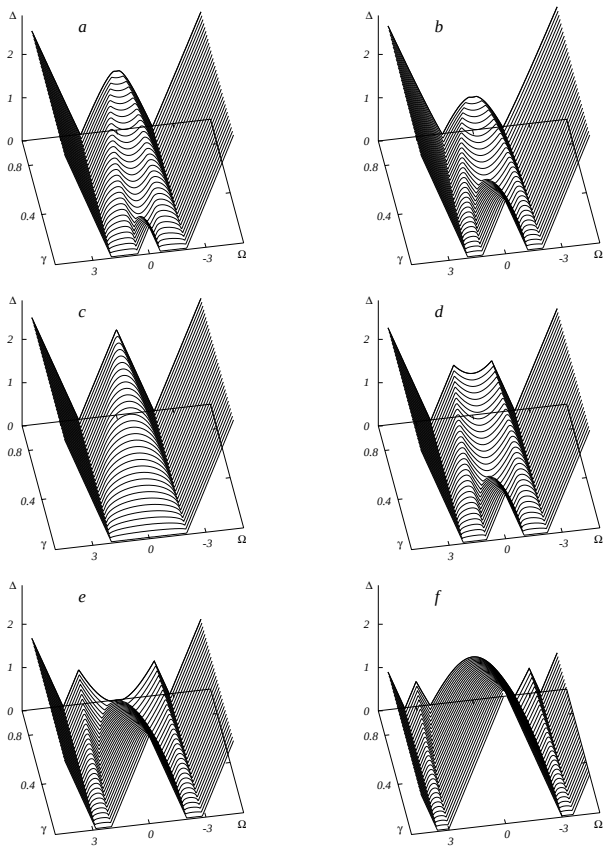


Figure 2. The energy gap $\Delta$ vs. transverse field $\Omega$ for spin–$\frac{1}{2}$ $XY$ chains of period 2 ($\Omega_{1,2} = \Omega$, $I_{1,2} = 1 \pm \Delta I$, $\Delta I = 0.3$ (a), $\Delta I = 0.6$ (b); $I_{1,2} = 1$, $\Omega_{1,2} = \Omega \pm \Delta\Omega$, $\Delta\Omega = 0$ (c), $\Delta\Omega = 1$ (d), $\Delta\Omega = 2$ (e), $\Delta\Omega = 3$ (f)). The results for the transverse Ising chain are compared with the results for an anisotropic $XY$ chain (with $2I_n\left((1+\gamma)s_n^x s_{n+1}^x + (1-\gamma)s_n^y s_{n+1}^y\right)$ instead of $2I_n s_n^x s_{n+1}^x$ in Eq. (2.1)) as $\gamma$ varies from 1 (transverse Ising chain with the exchange interaction $4I_n$) to 0 (transverse $XX$ chain with the exchange interaction $2I_n$).

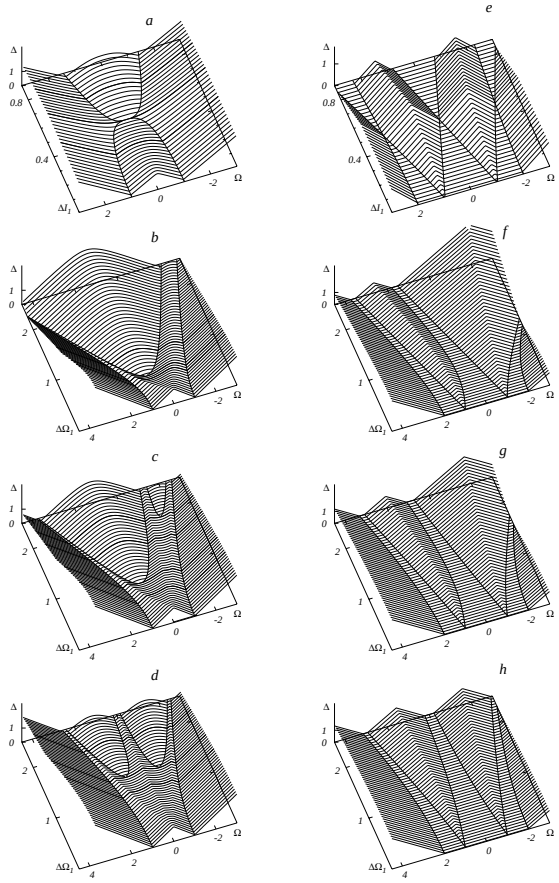


Figure 3. The energy gap $\Delta$ vs. transverse field $\Omega$ for spin–$\frac{1}{2}$ $XY$ chains of period 3 (a – d: transverse Ising chains, e – h: transverse $XX$ chains; $\Omega_{1,2,3} = \Omega + \Delta\Omega_{1,2,3}$, $\Delta\Omega_1 + \Delta\Omega_2 + \Delta\Omega_3 = 0$, $I_{1,2,3} = 1 + \Delta I_{1,2,3}$, $\Delta I_1 + \Delta I_2 + \Delta I_3 = 0$; $\Delta\Omega_{1,2,3} = 0$, $\Delta I_2 = \Delta I_1$ (a, e); $\Delta I_{1,2,3} = 0$, $\Delta\Omega_2 = \Delta\Omega_1$ (b, f), $\Delta\Omega_2 = \frac{1}{2}\Delta\Omega_1$ (c, g), $\Delta\Omega_2 = -\Delta\Omega_1$ (d, h)). The bold curves $\Delta$ vs. $\Omega$ correspond to the following values of parameters: $\Delta I = 0.3,\ 0.5,\ 0.7$ (panel a), $\Delta\Omega_1 = 0.5$, $\Delta\Omega_1 \approx 0.630$, $\Delta\Omega_1 = 1$ (panel b), $\Delta\Omega_1 = 0.5$, $\Delta\Omega_1 \approx 0.848$, $\Delta\Omega_1 = 1.5$, $\Delta\Omega_1 \approx 1.921$ (panel c), $\Delta\Omega_1 = 1$, $\Delta\Omega_1 \approx 1.375$, $\Delta\Omega_1 = 2$ (panel d). The bold curves in the planes $\Omega$–$\Delta I_1$ and $\Omega$–$\Delta\Omega_1$ indicate the values of parameters of transverse Ising chains (the boundaries of the region of parameters of transverse $XX$ chains) which yield the zero–energy gap, $\Delta = 0$.



for different values of the anisotropy parameter $\gamma$ which varies between $\gamma = 0$ ($XX$ interaction) and $\gamma = 1$ (Ising interaction) as it follows from (3.18). The results for transverse $XX$ chains in Figs. 1, 3 are obtained with the help of continued fractions [23]. In Figs. 2a, 2b one can see that $\Delta = 0$ for $\gamma = \pm\delta$, $\Omega = 0$ in agreement with [11, 15]. Let us also note a similarity between vanishing gap behaviour owing to anisotropy $\gamma$ in the case $\Delta I \neq 0$, $\Delta\Omega = 0$ seen in Figs. 2a and 2b (the case discussed in Refs. [15, 16]) and in the case $\Delta\Omega \neq 0$, $\Delta I = 0$ seen in Figs. 2d and 2e. From Refs. [11,15,16] we know that the presence of anisotropy or regular alternation of the exchange interaction makes the $XX$ chain (without transverse field) gapped, however, if they are present simultaneously the chain may become gapless. As we see from Figs. 2d, 2e the presence of exchange interaction anisotropy or of regularly alternating transverse field also makes the chain gapped, however, if they are present simultaneously the chain again may become gapless.

The vanishing gap indicates quantum phase transition points [4]. As can be seen from the data reported in the left panels in Figs. 1, 3 the number of such quantum phase transition points for a given period of alternation is strongly parameter–dependent. Thus the chains of period 2 may become gapless either at one, two, three, or four values of the transverse field, whereas the chains of period 3 may become gapless either at one, two, three, four, five, or six values of the transverse field depending on the concrete set of the Hamiltonian parameters (see Figs. 1 and 3). The condition for vanishing gap follows from $\mathcal{B}(0) = 0$ (3.16) ($\mathcal{C}(0) = 0$ (3.17)) and for the chains of period 2 (3) it reads $\Omega_1\Omega_2 = \pm I_1 I_2$ ($\Omega_1\Omega_2\Omega_3 = \pm I_1 I_2 I_3$). In fact we have rederived with the help of continued fractions the long known condition for existence of the zero–energy excitations in the inhomogeneous spin–$\frac{1}{2}$ transverse Ising chain [24] which in our notations has the form

$$\Omega_1\Omega_2\ldots\Omega_N = \pm I_1 I_2 \ldots I_N. \tag{3.20}$$

(Notice, that Eq. (6) of Ref. [24] does not contain two signs; the minus sign follows from the symmetry arguments after performing simple rotations of spin axes. It is important as will be seen below to have two signs in (3.20).) Obviously, for periodic chains we have the products of only $p$ multipliers in the l.h.s. and r.h.s. of Eq. (3.20).

For a chain of period 2 with a uniform transverse field Eq. (3.20) yields either one critical field $\Omega^\star = 0$ if either $I_1$ or $I_2$ (or both) equals to zero or two critical fields $\Omega^\star = \pm\sqrt{|I_1 I_2|}$ (see Fig. 1a). If the transverse field becomes regularly varying, $\Omega_{1,2} = \Omega \pm \Delta\Omega$, $\Delta\Omega > 0$, there may be either two critical fields $\Omega^\star = \pm\sqrt{\Delta\Omega^2 + |I_1 I_2|}$ if $\Delta\Omega < \sqrt{|I_1 I_2|}$,

or three critical fields $\Omega^\star = \left\{\pm\sqrt{2|I_1 I_2|}, 0\right\}$ if $\Delta\Omega = \sqrt{|I_1 I_2|}$, or four critical fields $\Omega^\star = \pm\sqrt{\Delta\Omega^2 \pm |I_1 I_2|}$ if $\Delta\Omega > \sqrt{|I_1 I_2|}$ (see Figs. 1b, 1c). As a result a chain of period 2 with $\Delta\Omega < \sqrt{|I_1 I_2|}$ as $\Omega$ varies exhibits two phases: the Ising phase (for $|\Omega| < \sqrt{\Delta\Omega^2 + |I_1 I_2|}$) and the paramagnetic phase (for $|\Omega| > \sqrt{\Delta\Omega^2 + |I_1 I_2|}$). A chain of period 2 with $\Delta\Omega = \sqrt{|I_1 I_2|}$ as $\Omega$ varies exhibits also two phases: the Ising phase (for $0 < |\Omega| < \sqrt{2|I_1 I_2|}$) and the paramagnetic phase (for $|\Omega| > \sqrt{2|I_1 I_2|}$); moreover, in the Ising phase at $\Omega = \Omega^\star = 0$ the system exhibits a weak singularity in the ground–state quantities (see below). A chain of period 2 with $\Delta\Omega > \sqrt{|I_1 I_2|}$ as $\Omega$ varies exhibits three phases: the low–field paramagnetic phase (for $|\Omega| < \sqrt{\Delta\Omega^2 - |I_1 I_2|}$), the Ising phase (for $\sqrt{\Delta\Omega^2 - |I_1 I_2|} < |\Omega| < \sqrt{\Delta\Omega^2 + |I_1 I_2|}$), and the high–field paramagnetic phase (for $|\Omega| > \sqrt{\Delta\Omega^2 + |I_1 I_2|}$). A motivation to give such names to different phases follows from a behaviour of the Ising magnetization $m^x$ to be discussed below in Section 4.

For a chain of period 3 ($\Omega_{1,2,3} = \Omega + \Delta\Omega_{1,2,3}$, $\Delta\Omega_1 + \Delta\Omega_2 + \Delta\Omega_3 = 0$) the critical fields follow from two cubic equations

$$(\Omega^\star + \Delta\Omega_1)\,(\Omega^\star + \Delta\Omega_2)\,(\Omega^\star + \Delta\Omega_3) \pm I_1 I_2 I_3 = 0 \qquad (3.21)$$

each of which may have either one real solution or three real solutions. In Fig. 4 we display the regions in $\Delta\Omega_1$–$\Delta\Omega_2$ plane for the set of parameters of the transverse Ising chains with $|I_1 I_2 I_3| = 1$ which yield two (dark region), four (grey region), or six (light region) values of the critical field. For the set of parameters at the boundary between dark and grey (grey and light) regions there are three (five) critical fields; for the set of parameters where dark, grey and light regions meet there are four critical fields. The behaviour of the energy gap for all cases can be seen in Fig. 3. As a result the chain of period 3 depending on a relation between $\Delta\Omega_1$, $\Delta\Omega_2$, $\Delta\Omega_3$ may exhibit either two phases (the Ising and paramagnetic phases), or four phases (two Ising and two paramagnetic phases), or six phases (three Ising and three paramagnetic phases). Moreover, weak singularities in the Ising phases may occur.

Further discussion of the quantum phase transitions (critical behaviour, spin correlations and order parameter behaviour) is given in Section 4.



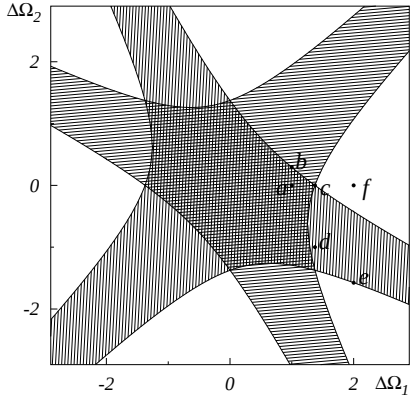


Figure 4. Phase diagram of the transverse Ising chain of period 3 with $|I_1 I_2 I_3| = 1$, $\Omega_{1,2,3} = \Omega + \Delta\Omega_{1,2,3}$, $\Delta\Omega_1 + \Delta\Omega_2 + \Delta\Omega_3 = 0$. As $\Omega$ varies the energy gap vanishes two/four/six times if the set of parameters is in the dark/grey/light region. The sets of parameters denoted by a, b, c, d, e, f are used below to illustrate the dependence on $\Omega$ of the ground–state Ising magnetization and the low–temperature specific heat.

## 4. The ground–state magnetic properties

### 4.1. Strong–coupling limit

We pass to the magnetic properties of regularly alternating spin chains. Although the transverse magnetization and the static transverse susceptibility for the general case immediately follow from Eqs. (3.14) and (3.15) if the density of states $R(E^2)$ (3.10) is known we begin with a particular case of a regularly alternating chain having one zero exchange interaction (without loss of generality we assume $I_p = 0$). Such a simple case already indicates the peculiarities of the low–temperature magnetization curves (and other thermodynamic quantities, see Section 5) which obviously become modified as $I_p$ deviates from zero. Another outcome of this consideration is the exact ground–state eigenvector for a general regularly alternating transverse Ising chain at certain values of the transverse field. If $I_p = 0$ the chain splits into noninteracting clusters each with the Hamiltonian $H_p = \Omega_1 s_1^z + \ldots + \Omega_p s_p^z + 2I_1 s_1^x s_2^x + \ldots + 2I_{p-1} s_{p-1}^x s_p^x$. Such a chain arises within the strong–coupling approach treatment (which is usually applied to more complicated spin systems) when at

first the smallest interaction is assumed to be zero and then it is taking into account as perturbation. The equilibrium properties of the chain in the strong–coupling limit can be analyzed in detail using the exact eigenvalues and eigenvectors of the $p$–site cluster Hamiltonian $H_p$. For example, the ground–state transverse magnetization of the chain per site is $m^z = \frac{1}{p}\langle \mathrm{GS}|s_1^z + \ldots + s_p^z|\mathrm{GS}\rangle$ where $|\mathrm{GS}\rangle$ is the ground–state eigenvector of $H_p$, $\langle \mathrm{GS}|\mathrm{GS}\rangle = 1$. The ground–state eigenvectors of the 2– and 3–site cluster Hamiltonians of the anisotropic $XY$ model in a uniform transverse field were considered in Ref. [14] (see also Ref. [25]).

In the case of 2–site cluster Hamiltonian with the parameters $\Omega_1 I_1 \Omega_2$ the coefficients determining four eigenvectors

$$|\psi\rangle = c_1|\downarrow_1\downarrow_2\rangle + c_2|\downarrow_1\uparrow_2\rangle + c_3|\uparrow_1\downarrow_2\rangle + c_4|\uparrow_1\uparrow_2\rangle, \quad \langle\psi|\psi\rangle = 1$$

and the corresponding eigenvalues $E$ are collected in Table 4.1. In the last column of Table 4.1 we give the transverse magnetization in different eigenstates. In the case of uniform field, $\Delta\Omega = 0$, the ground state is given by $c_1, \ldots, c_4$ from the first row in Table 4.1 for any $\Omega$ and as a result $m^z$ vs. $\Omega$ is a smoothly varying curve. If $\Delta\Omega \neq 0$ there is a change in the ground state as $\Omega$ varies. Until $|\Omega| < \Delta\Omega$ the ground state is given by $c_1, \ldots, c_4$ from the second row in Table 4.1 whereas as $|\Omega|$ exceeds $\Delta\Omega$ the ground state is given by $c_1, \ldots, c_4$ from the first row in Table 4.1. As a result $m^z = 0$ until $|\Omega| < \Delta\Omega$ and then it jumps to a certain nonzero value and further increases its value approaching $\frac{1}{2}$ as $|\Omega|$ exceeds $\Delta\Omega$ and further increases. In Fig. 5 we show the dependences of the eigenvalues of 2–site cluster Hamiltonian and the transverse magnetizations in different states on $\Omega$. Note, that in the strong–coupling limit Eq. (3.20) yields $\Omega_1 \ldots \Omega_p = 0$ and hence there are, generally speaking, $p$ critical fields $-\Delta\Omega_1, \ldots, -\Delta\Omega_p$ which can be seen in Fig. 5 in the case $p = 2$ (and in Fig. 6 in the case $p = 3$). In Fig. 5 (and Fig. 6) we also compare the results for the transverse Ising (left panels) and transverse $XX$ (right panels) models.

In the case of 3–site cluster Hamiltonian with the parameters $\Omega_1 I_1 \Omega_2 I_2 \Omega_3$ we seek for four sets of coefficients $c_1$, $c_5$, $c_6$, $c_7$ and four



Table 4.1. The eigenvalues $E$, eigenvectors $|\psi\rangle$ and the transverse magnetization $\frac{1}{p}\langle\psi|\sum_n s_n^z|\psi\rangle$ for the 2–site cluster Hamiltonian of the Ising model in a transverse field; $c_\pm = \sqrt{(\Omega_1 \pm \Omega_2)^2 + {I_1}^2}$.

| $E$ | $c_1$ | $c_2$ | $c_3$ | $c_4$ | $\frac{1}{2}\langle\psi\|s_1^z + s_2^z\|\psi\rangle$ |
|---|---|---|---|---|---|
| $-\frac{1}{2}c_+$ | $\frac{\Omega_1+\Omega_2+c_+}{\sqrt{2c_+(c_++\Omega_1+\Omega_2)}}$ | 0 | 0 | $-\frac{I_1}{\sqrt{2c_+(c_++\Omega_1+\Omega_2)}}$ | $-\frac{\Omega_1+\Omega_2}{2c_+}$ |
| $-\frac{1}{2}c_-$ | 0 | $\frac{\Omega_1-\Omega_2+c_-}{\sqrt{2c_-(c_-+\Omega_1-\Omega_2)}}$ | $-\frac{I_1}{\sqrt{2c_-(c_-+\Omega_1-\Omega_2)}}$ | 0 | 0 |
| $\frac{1}{2}c_-$ | 0 | $\frac{\Omega_1-\Omega_2-c_-}{\sqrt{2c_-(c_--\Omega_1+\Omega_2)}}$ | $-\frac{I_1}{\sqrt{2c_-(c_--\Omega_1+\Omega_2)}}$ | 0 | 0 |
| $\frac{1}{2}c_+$ | $\frac{\Omega_1+\Omega_2-c_+}{\sqrt{2c_+(c_+-\Omega_1-\Omega_2)}}$ | 0 | 0 | $-\frac{I_1}{\sqrt{2c_+(c_+-\Omega_1-\Omega_2)}}$ | $\frac{\Omega_1+\Omega_2}{2c_+}$ |

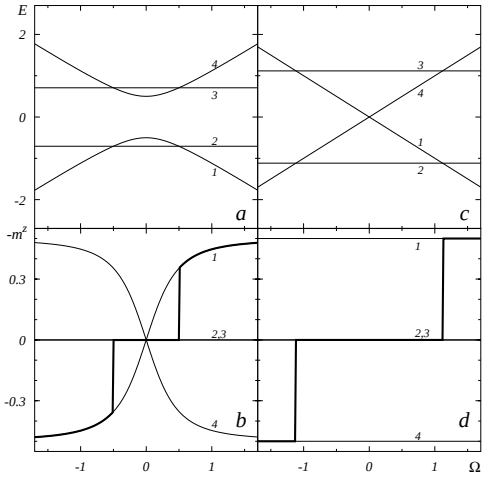


Figure 5. 2–site cluster energies (a, c) and transverse magnetizations in different states (b, d) for the transverse Ising (a, b) and transverse $XX$ (c, d) Hamiltonians ($I_1 = 1$, $I_2 = 0$, $\Omega_{1,2} = \Omega \pm 0.5$). The bold curves in panels b and d indicate the ground–state magnetization curves.

sets of coefficients $c_2$, $c_3$, $c_4$, $c_8$ which determine eight eigenvectors

$$|\psi\rangle = \sum_{l=1}^{8} c_l |l_{123}\rangle,$$

$$|1_{123}\rangle = |\downarrow_1\downarrow_2\downarrow_3\rangle, \quad |2_{123}\rangle = |\downarrow_1\downarrow_2\uparrow_3\rangle,$$
$$|3_{123}\rangle = |\downarrow_1\uparrow_2\downarrow_3\rangle, \quad |4_{123}\rangle = |\uparrow_1\downarrow_2\downarrow_3\rangle,$$
$$|5_{123}\rangle = |\downarrow_1\uparrow_2\uparrow_3\rangle, \quad |6_{123}\rangle = |\uparrow_1\downarrow_2\uparrow_3\rangle,$$
$$|7_{123}\rangle = |\uparrow_1\uparrow_2\downarrow_3\rangle, \quad |8_{123}\rangle = |\uparrow_1\uparrow_2\uparrow_3\rangle,$$
$$\langle\psi|\psi\rangle = 1$$

and the corresponding eigenvalues $E$. The transverse magnetization in a certain eigenstate is given by

$$m^z = \frac{1}{6}\left(-3c_1^2 - c_2^2 - c_3^2 - c_4^2 + c_5^2 + c_6^2 + c_7^2 + 3c_8^2\right).$$

In Fig. 6 we plot such results for a typical set of parameters of 3–site cluster Hamiltonian.

Employing the unitary transformation which interchanges fields and interactions (see Section 2) we can use the cluster Hamiltonian eigenvectors to obtain the eigenvectors of the chains like $\Omega_1 I_1 0 I_2 \Omega_1 I_1 0 I_2 \ldots$



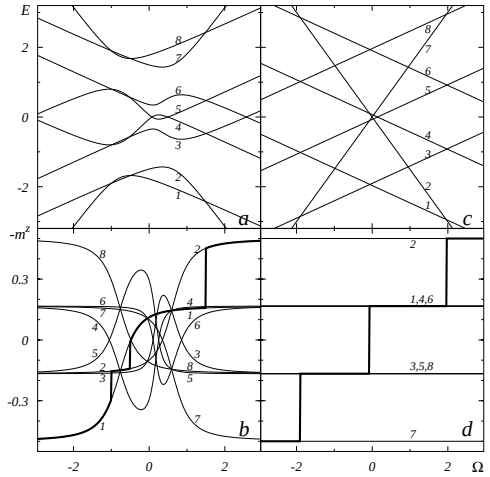


Figure 6. 3–site cluster energies (a, c) and transverse magnetizations in different states (b, d) for the transverse Ising (a, b) and transverse $XX$ (c, d) Hamiltonians ($I_{1,2} = 1$, $I_3 = 0$, $\Omega_1 = \Omega + 1$, $\Omega_2 = \Omega + 0.5$, $\Omega_3 = \Omega - 1.5$). The bold curves in panels b and d indicate the ground–state magnetization curves.

($p = 2$), $\Omega_1 I_1 \Omega_2 I_2 0 I_3 \Omega_1 I_1 \Omega_2 I_2 0 I_3 \ldots$ ($p = 3$) etc.. Thus, for a chain of period 2, $\Omega_1 I_1 \Omega_2 I_2 \Omega_1 I_1 \Omega_2 I_2 \ldots$ , with $I_1 I_2 > 0$ and $\Omega_n = 0$, $\Omega_{n+1} = -2\Delta\Omega$ we get

$$|\mathrm{GS}\rangle = U^+ R^{z+} \ldots (c_1|\downarrow_{n+1}\downarrow_{n+2}\rangle + c_4|\uparrow_{n+1}\uparrow_{n+2}\rangle) \cdot (c_1|\downarrow_{n+3}\downarrow_{n+4}\rangle + c_4|\uparrow_{n+3}\uparrow_{n+4}\rangle)\ldots \qquad (4.1)$$

where $U$ and $R^z$ are given in Section 2 and $c_1$, $c_4$ follows from the formulas in the first row in Table 4.1 after the substitution $\Omega_1 \to I_1$, $I_1 \to -2\Delta\Omega$, $\Omega_2 \to I_2$. For another value of the transverse field when $\Omega_n = 2\Delta\Omega$, $\Omega_{n+1} = 0$ the ground state is again given by (4.1) with $n \to n-1$, $\Delta\Omega \to -\Delta\Omega$ (see [26]). If $I_1 I_2 < 0$ and $\Omega_n = 0$, $\Omega_{n+1} = -2\Delta\Omega$ we have

$$|\mathrm{GS}\rangle = U^+ R^{z+} \ldots (c_2|\downarrow_{n+1}\uparrow_{n+2}\rangle + c_3|\uparrow_{n+1}\downarrow_{n+2}\rangle) \cdot (c_2|\downarrow_{n+3}\uparrow_{n+4}\rangle + c_3|\uparrow_{n+3}\downarrow_{n+4}\rangle)\ldots \qquad (4.2)$$

and $c_2$, $c_3$ follows from the formulas in the second row in Table 4.1 after the substitution $\Omega_1 \to I_1$, $I_1 \to -2\Delta\Omega$, $\Omega_2 \to I_2$. For another value of the transverse field when $\Omega_n = 2\Delta\Omega$, $\Omega_{n+1} = 0$ the ground state is again given by (4.2) with $n \to n-1$, $\Delta\Omega \to -\Delta\Omega$. Similarly, for the

chain of period 3, $\Omega_1 I_1 \Omega_2 I_2 \Omega_3 I_3 \Omega_1 I_1 \Omega_2 I_2 \Omega_3 I_3 \dots$, with $\Omega_n = \Omega_1 = 0$, $\Omega_{n+1} = \Omega_2 = -\Delta\Omega_1 + \Delta\Omega_2$, $\Omega_{n+2} = \Omega_3 = -2\Delta\Omega_1 - \Delta\Omega_2$ we find

$$|\mathrm{GS}\rangle = U^+ R^{z+} \dots \left( \sum_{l=1}^{8} c_l |l_{n+1,n+2,n+3}\rangle \right) \cdot \left( \sum_{l=1}^{8} c_l |l_{n+4,n+5,n+6}\rangle \right) \dots \tag{4.3}$$

where the coefficients $c_l$ determine the ground state of the 3–site cluster Hamiltonian $I_1 \Omega_2 I_2 \Omega_3 I_3$. For example, if $I_1 = I_2 = I_3 = 1$, $\Delta\Omega_1 = 1(2)$, $\Delta\Omega_2 = 0$ and $\Omega = -1(-2)$ we get

$$c_1 \approx 0.880(0.737),\ c_5 \approx 0.376(0.474),\ c_6 \approx 0.166(0.318),$$
$$c_7 \approx 0.237(0.363),\ c_2 = c_3 = c_4 = c_8 = 0(0).$$

To get the ground state for the chain with $\Omega_n = \Omega_1 = \Delta\Omega_1 - \Delta\Omega_2$, $\Omega_{n+1} = \Omega_2 = 0$, $\Omega_{n+2} = \Omega_3 = -\Delta\Omega_1 - 2\Delta\Omega_2$ ($\Omega_n = \Omega_1 = 2\Delta\Omega_1 + \Delta\Omega_2$, $\Omega_{n+1} = \Omega_2 = \Delta\Omega_1 + 2\Delta\Omega_2$, $\Omega_{n+2} = \Omega_3 = 0$) one should make in Eq. (4.3) the change $n \to n+1$, $I_1 \Omega_2 I_2 \Omega_3 I_3 \to I_2 \Omega_3 I_3 \Omega_1 I_1$ ($n \to n+2$, $I_1 \Omega_2 I_2 \Omega_3 I_3 \to I_3 \Omega_1 I_1 \Omega_2 I_2$).

Knowing the ground state one can calculate the ground–state spin correlation functions employing the relations

$$\begin{aligned} R^z U s_n^x U^+ R^{z+} &= -s_1^y \left(2s_2^z\right) \dots \left(2s_{n-1}^z\right) \left(2s_n^z\right), \\ R^z U s_n^y U^+ R^{z+} &= s_1^y \left(2s_2^z\right) \dots \left(2s_{n-1}^z\right) \left(2s_n^y\right) \left(2s_{n+1}^x\right), \\ R^z U s_n^z U^+ R^{z+} &= 2 s_n^x s_{n+1}^x. \end{aligned} \tag{4.4}$$

For example, for the chain of period 3, $\Omega_1 I_1 \Omega_2 I_2 \Omega_3 I_3 \Omega_1 I_1 \Omega_2 I_2 \Omega_3 I_3 \dots$, with $\Omega_n = \Omega_1 = 0$, $\Omega_{n+1} = \Omega_2 = -\Delta\Omega_1 + \Delta\Omega_2$, $\Omega_{n+2} = \Omega_3 = -2\Delta\Omega_1 - \Delta\Omega_2$ we have

$$\begin{aligned} 4\langle s_{n+1}^x s_{n+2}^x \rangle &= C, \quad 4\langle s_{n+1}^x s_{n+5+3k}^x \rangle = I T^k E, \\ 4\langle s_{n+1}^x s_{n+3+3k}^x \rangle &= I T^k, \quad 4\langle s_{n+1}^x s_{n+4+3k}^x \rangle = I T^k L, \\ 4\langle s_{n+2}^x s_{n+3+3k}^x \rangle &= R T^k, \quad 4\langle s_{n+2}^x s_{n+4+3k}^x \rangle = R T^k L, \\ 4\langle s_{n+2}^x s_{n+5+3k}^x \rangle &= R T^k E, \quad 4\langle s_{n+3}^x s_{n+4+3k}^x \rangle = T^k L, \\ 4\langle s_{n+3}^x s_{n+5+3k}^x \rangle &= T^k E, \quad 4\langle s_{n+3}^x s_{n+3+3k}^x \rangle = T^k, \end{aligned} \tag{4.5}$$



$k = 0, 1, 2, \dots$ with

$$\begin{aligned} L &= -c_1^2 - c_2^2 - c_3^2 + c_4^2 - c_5^2 + c_6^2 + c_7^2 + c_8^2, \\ C &= -c_1^2 - c_2^2 + c_3^2 - c_4^2 + c_5^2 - c_6^2 + c_7^2 + c_8^2, \\ R &= -c_1^2 + c_2^2 - c_3^2 - c_4^2 + c_5^2 + c_6^2 - c_7^2 + c_8^2, \\ E &= c_1^2 + c_2^2 - c_3^2 - c_4^2 - c_5^2 - c_6^2 + c_7^2 + c_8^2, \\ I &= c_1^2 - c_2^2 - c_3^2 + c_4^2 + c_5^2 - c_6^2 - c_7^2 + c_8^2, \\ T &= -c_1^2 + c_2^2 + c_3^2 + c_4^2 - c_5^2 - c_6^2 - c_7^2 + c_8^2. \end{aligned} \tag{4.6}$$

Since $|T^k| = 1$ the two–spin correlations are independent on the inter-site distance. In the end of this Section we compare these analytical predictions with numerics (available for an arbitrary transverse field).

### 4.2. Transverse Ising chain vs. transverse $XX$ chain

As have been mentioned before the transverse magnetization and the static transverse susceptibility for an arbitrary regularly alternating transverse Ising chain (Eqs. (3.14), (3.15)) can be obtained using continued fractions. Such results for some typical chains of period 2 and 3 (which roughly correspond to the parameters singled out in Figs. 1 and 3) at zero temperature are reported in Figs. 7 and 8, respectively. Below we compare and contrast the results for the magnetic properties of the transverse Ising and the transverse $XX$ chains which are shown in Figs. 1 – 3, 5 – 8.

We start from the energy gap. It is known that the uniform transverse Ising chain becomes gapless at critical field $\Omega^\star = \pm|I|$. The gap decays linearly while the transverse field approaches the critical value, $\Delta \sim \epsilon$, $\epsilon = |\Omega - \Omega^\star| \to 0$. The transverse $XX$ chain is gapless along the critical line $-|I| \le \Omega \le |I|$. The gap opens linearly while the value of transverse field exceeds $|I|$. For an arbitrary small amount of anisotropy $\gamma$ the critical line transforms into two critical points (Fig. 2c). If regular inhomogeneity is introduced into the transverse $XX$ chain the critical line splits into several part; the gaps open linearly as the transverse field runs out the critical lines (Figs. 1d – 1f, 3e – 3h). Contrary, a regular inhomogeneity introduced into the transverse Ising chain may either only shift the values of critical fields or lead to appearance of new critical points. Moreover, the gap decays either linearly, $\Delta \sim \epsilon$, or proportionally to the deviation from the critical value squared, $\Delta \sim \epsilon^2$, as can be seen in Figs. 1a – 1c, 3a – 3d). The case $p = 2$ was discussed by several authors in more detail. In particular, in Ref. [16] for a chain with the anisotropic $XY$ exchange interaction $(1 + \gamma + (-1)^n \delta)\, s_n^x s_{n+1}^x + (1 - \gamma + (-1)^n \delta)\, s_n^y s_{n+1}^y$

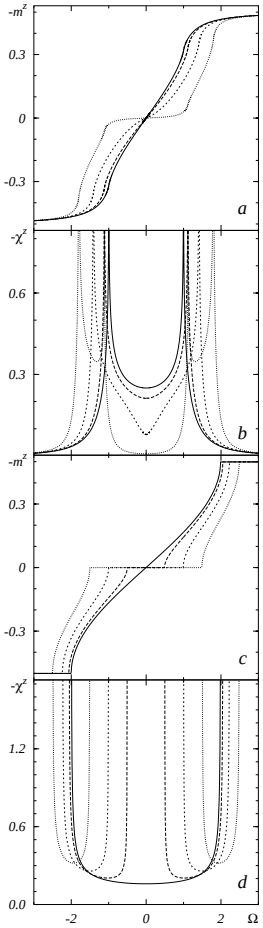


Figure 7. The ground–state transverse magnetization (a, c) and static transverse susceptibility (b, d) curves for transverse Ising (a, b) and transverse $XX$ (c, d) chains of period $p = 2$. $I_{1,2} = 1$, $\Omega_{1,2} = \Omega \pm \Delta\Omega$, $\Delta\Omega = 0$ (solid curves), $\Delta\Omega = 0.5$ (long–dashed curves), $\Delta\Omega = 1$ (short–dashed curves), $\Delta\Omega = 1.5$ (dotted curves).



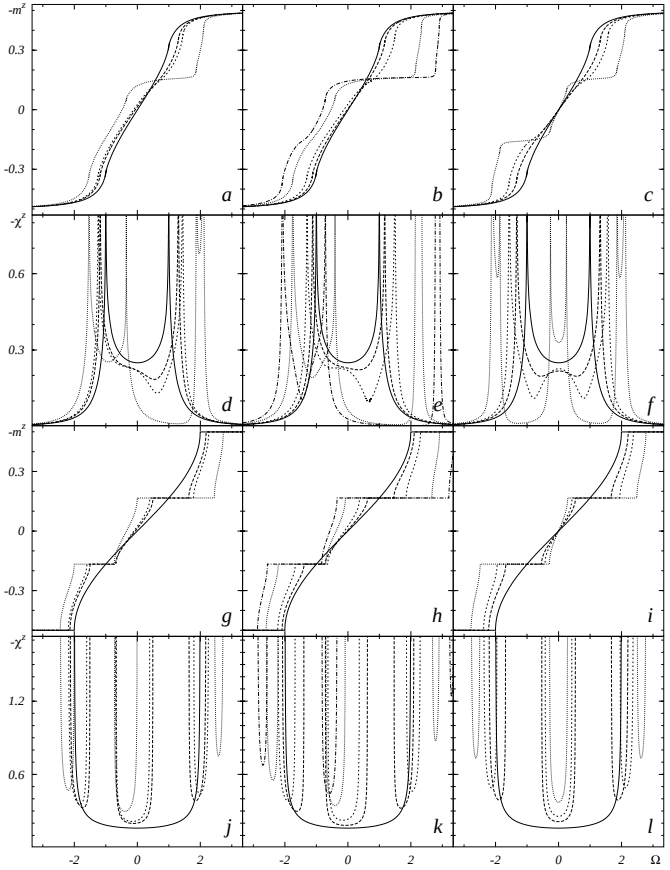


Figure 8. The ground–state transverse magnetization (a, b, c, g, h, i) and static transverse susceptibility (d, e, f, j, k, l) curves for transverse Ising (a – f) and transverse $XX$ (g – l) chains of period $p = 3$. $I_{1,2,3} = 1$, $\Omega_{1,2,3} = \Omega + \Delta\Omega_{1,2,3}$, $\Delta\Omega_1 + \Delta\Omega_2 + \Delta\Omega_3 = 0$; a, d, g, j: $\Delta\Omega_2 = \Delta\Omega_1$, $\Delta\Omega_1 = 0$ (solid curves), $\Delta\Omega_1 = 0.5$ (long–dashed curves), $\Delta\Omega_1 = 0.6$ (short–dashed curves), $\Delta\Omega_1 = 1$ (dotted curves); b, e, h, k: $\Delta\Omega_2 = \frac{1}{2}\Delta\Omega_1$, $\Delta\Omega_1 = 0$ (solid curves), $\Delta\Omega_1 = 0.5$ (long–dashed curves), $\Delta\Omega_1 = 0.85$ (short–dashed curves), $\Delta\Omega_1 = 1.5$ (dotted curves), $\Delta\Omega_1 = 1.9$ (long–dashed–dotted curves); c, f, i, l: $\Delta\Omega_2 = -\Delta\Omega_1$, $\Delta\Omega_1 = 0$ (solid curves), $\Delta\Omega_1 = 1$ (long–dashed curves), $\Delta\Omega_1 = 1.35$ (short–dashed curves), $\Delta\Omega_1 = 2$ (dotted curves).

the critical fields where the chain becomes gapless are given as $\Omega^\star = \pm\sqrt{\delta^2-\gamma^2}$. Further the authors of Ref. [16] consider as an example the case $\delta = 0.3$, $\gamma = 0.1$ (Fig. 1 of that paper), i.e., the case when gap vanishes linearly $\sim \epsilon$. Another case of the dimerized anisotropic $XY$ chain in a transverse field when the gap vanishes $\sim \epsilon^2$ (see Figs. 2a, 2b) was not discussed in Ref. [16].

The energy gap behaviour determines the zero–temperature transverse magnetization curves for both chains. Transverse $XX$ chains exhibit plateaus which can be easily understood within the frames of fermionic picture. Indeed, a regularly alternating transverse $XX$ chain corresponds to a system of free fermions with several energy bands and the transverse field plays the role of the chemical potential. Transverse Ising chains do not exhibit plateaus, however, being in the paramagnetic phases exhibit plateau–like steps (compare the curves in Fig. 7a and in Fig. 1c, and in Figs. 8a – 8c and in Figs. 3b – 3d). In the Ising phases the transverse magnetization shows rapid change. In the fermionic picture a regularly alternating transverse Ising chain again corresponds to a system of free fermions with several energy bands, however, the transverse field does not play the role of the chemical potential any more.

The described behaviour of the transverse magnetization vs. transverse field is accompanied by the corresponding peculiarities in the behaviour of the static transverse susceptibility vs. transverse field. Thus, in the cases of the transverse $XX$ chain the square–root singularities indicate the gapless–to–gapped transitions. In the case of the transverse Ising chain a linear gap decay produces a logarithmic singularity, whereas for a decay proportional to the squared deviation from the critical value the static transverse susceptibility does not diverge containing, however, a nonanalytical contribution which causes a logarithmic singularity of its second derivative (see short–dashed curve in Fig. 7b, and short–dashed and long–dashed–dotted curves in Figs. 8d – 8f).

To end up, we emphasize that for the regularly alternating transverse $XX$ chains the number of peculiarities (e.g., in the dependence $\chi^z$ vs. $\Omega$) depends only on the period of alternation and equals $2p$. This is not the case for the regularly alternating transverse Ising chains: the number of peculiarities can not exceed $2p$ but may be smaller; the actual number of peculiarities and their type essentially depends on the concrete set of the Hamiltonian parameters. Let us also underline a similarity of these results with what has been found for the anisotropic/isotropic $XY$ models on one–dimensional superlattices [13, 14, 27].



### 4.3. Quantum chain vs. classical chain

Motivated by the difference between the zero–temperature magnetization processes in the regularly alternating transverse Ising and transverse $XX$ chains we consider the classical counterparts of these models (some calculations of the thermodynamic quantities of uniform classical spin chains can be found in Ref. [28]) to demonstrate the role of quantum effects. The classical spin model consists of classical spins (vectors) $\mathbf{s} = (s, \theta, \phi)$ ($0 \le \theta \le \pi$ and $0 \le \phi < 2\pi$ are the spherical coordinates of the spin) on a ring which interact with each other and an external field and are governed either by the Hamiltonian

$$H = \sum_{n=1}^{N} \Omega_n s \cos\theta_n + \sum_{n=1}^{N} 2I_n s^2 \sin\theta_n \sin\theta_{n+1} \cos\phi_n \cos\phi_{n+1}, \quad \mathbf{s}_{N+1} = \mathbf{s}_1 \tag{4.7}$$

(transverse Ising chain) or by the Hamiltonian

$$H = \sum_{n=1}^{N} \Omega_n s \cos\theta_n + \sum_{n=1}^{N} 2I_n s^2 \sin\theta_n \sin\theta_{n+1} \cos\left(\phi_n - \phi_{n+1}\right), \quad \mathbf{s}_{N+1} = \mathbf{s}_1 \tag{4.8}$$

(transverse $XX$ chain). In Eqs. (4.7), (4.8) $s$ is the value of spin which plays only a quantitative role (further we put $s = \frac{1}{2}$) and the sequence of parameters for a regularly alternating chain of period $p$ is again $I_1\Omega_1 I_2\Omega_2 \ldots I_p\Omega_p I_1\Omega_1 I_2\Omega_2 \ldots I_p\Omega_p \ldots$. In what follows we restrict ourselves to the case $I_n = I$, $\Omega_n = \Omega + \Delta\Omega_n$, $\sum_n \Delta\Omega_n = 0$ which has been discussed already in some detail above. Our goal is to examine the influence of regular inhomogeneity on the ground–state properties of the classical transverse Ising and transverse $XX$ chains.

Consider at first the transverse Ising chain. One can easily construct the ground–state spin configuration and the corresponding ground–state energy ansatz. According to (4.7) to minimize the ground–state energy one should place all spins in $xz$ plane (i.e., $\phi_n = \phi_{n+1} = \ldots = 0(\pi)$ if $I < 0$ or $\phi_n = \phi_{n+2} = \ldots = 0$, $\phi_{n+1} = \phi_{n+3} = \ldots = \pi$ if $I > 0$). Moreover, the angles $\theta$s are determined to minimize the sum of the contribution coming from the interaction with the transverse field and of the contribution coming from the intersite interaction taking into account the period of inhomogeneity. Thus, for chains of periods 1, 2, 3 etc. an ansatz for the ground–state energy per site reads

$$\frac{E(\theta)}{N} = \Omega s \cos\theta - 2|I| s^2 \sin^2\theta, \tag{4.9}$$

$$\frac{E(\theta_1,\theta_2)}{N} = \frac{1}{2}s\left((\Omega+\Delta\Omega)\cos\theta_1 + (\Omega-\Delta\Omega)\cos\theta_2\right) - 2|I|s^2\sin\theta_1\sin\theta_2, \quad (4.10)$$

$$\frac{E(\theta_1,\theta_2,\theta_3)}{N} = \frac{1}{3}s\left((\Omega+\Delta\Omega_1)\cos\theta_1 + (\Omega+\Delta\Omega_2)\cos\theta_2 + (\Omega-\Delta\Omega_1-\Delta\Omega_2)\cos\theta_3\right) - \frac{2}{3}|I|s^2\left(\sin\theta_1\sin\theta_2+\sin\theta_2\sin\theta_3+\sin\theta_3\sin\theta_1\right) \quad (4.11)$$

etc. and the angles $\theta$s are determined from the sets of equations

$$\sin\theta\left(\Omega+4|I|s\cos\theta\right) = 0, \quad (4.12)$$

$$\begin{aligned}(\Omega+\Delta\Omega)\sin\theta_1 + 4|I|s\cos\theta_1\sin\theta_2 &= 0,\\ (\Omega-\Delta\Omega)\sin\theta_2 + 4|I|s\sin\theta_1\cos\theta_2 &= 0,\end{aligned} \quad (4.13)$$

$$\begin{aligned}(\Omega+\Delta\Omega_1)\sin\theta_1 + 2|I|s\cos\theta_1\left(\sin\theta_2+\sin\theta_3\right) &= 0,\\ (\Omega+\Delta\Omega_2)\sin\theta_2 + 2|I|s\cos\theta_2\left(\sin\theta_1+\sin\theta_3\right) &= 0,\\ (\Omega-\Delta\Omega_1-\Delta\Omega_2)\sin\theta_3 + 2|I|s\cos\theta_3\left(\sin\theta_1+\sin\theta_2\right) &= 0\end{aligned} \quad (4.14)$$

etc., respectively. Substituting the solution of Eqs. (4.12), (4.13), (4.14) (more precisely, the solution which yields the lowest ground–state energy) into Eq. (4.9), (4.10), (4.11), respectively, we get the ground–state energy of the corresponding chains. Now the ground–state on–site magnetizations are given by $m_n^z = s\cos\theta_n$, $m_n^x = s\sin\theta_n\cos\phi_n$. We can also find the ground–state on–site static transverse susceptibility $\chi_n^z = \frac{\partial m_n^z}{\partial\Omega}$.

Let us turn to the transverse $XX$ chain (4.8). In the ground–state spin configuration the spin components in $xy$ plane are directed arbitrarily but coherently at all sites having the values $\left|m_n^\perp\right| = s\sin\theta_n$ (i.e., $\phi_n = \phi_{n+1} = \ldots = \phi$ ($\phi$ is an arbitrary angle) if $I < 0$ or $\phi_n = \phi_{n+2} = \ldots = \phi$ ($0 \le \phi < \pi$), $\phi_{n+1} = \phi_{n+3} = \ldots = \phi + \pi$ if $I > 0$). An ansatz for the ground–state energy per site for the chains of period 1, 2, 3 is again given be Eqs. (4.9), (4.10), (4.11) and the angles $\theta$s are determined from Eqs. (4.12), (4.13), (4.14). Moreover, $m_n^z = s\cos\theta_n$ and $\chi_n^z = \frac{\partial m_n^z}{\partial\Omega}$.

For the chain of period 1 from (4.12) one easily finds

$$\theta = \begin{cases} 0, & \text{if } \omega < -1,\\ \arccos(-\omega), & \text{if } -1 \le \omega < 1,\\ \pi, & \text{if } 1 \le \omega; \end{cases} \quad (4.15)$$

$$\omega = \frac{\Omega}{4s|I|}.$$



For the chain of period 2 Eq. (4.13) in addition to four obvious solutions $\cos^2\theta_1 = \cos^2\theta_2 = 1$ one gets one more solution

$$\begin{aligned}\cos^2\theta_1 &= (\omega+\delta)^2\,\frac{1+(\omega-\delta)^2}{1+(\omega+\delta)^2},\\ \cos^2\theta_2 &= (\omega-\delta)^2\,\frac{1+(\omega+\delta)^2}{1+(\omega-\delta)^2};\\ \delta &= \frac{\Delta\Omega}{4s|I|}\end{aligned} \quad (4.16)$$

if $|\omega^2-\delta^2| \le 1$. Eq. (4.14) has again obvious solutions $\cos^2\theta_1 = \cos^2\theta_2 = \cos^2\theta_3 = 1$; another solution existing at a certain range of the transverse field can be found numerically. The described analytical calculations reproduce the results obtained earlier numerically for some chains of periods 2 and 3 (dashed curves in Figs. 8a, 8b of Ref. [23]).

In Figs. 9, 10 we display the obtained dependences of the ground–state magnetizations $m^z$, $m^x$ and static transverse susceptibility $\chi^z$ on the transverse field for several classical transverse Ising/$XX$ chains of periods 2 and 3 (the results for corresponding quantum chains are shown in Figs. 7, 8). In contrast to the quantum case, the ground–state static transverse susceptibility $\chi^z$ of the classical chains remains always finite as the transverse field $\Omega$ varies (Figs. 9b, 10d – 10f) and hence the classical chains do not exhibit any ground–state phase transitions driven by $\Omega$. However, it is interesting to note, that a regularly alternating classical chain similarly to its quantum ($XX$) counterpart may exhibit plateaus in the ground–state dependence transverse magnetization $m^z$ vs. transverse field $\Omega$ (compare long–dashed–dotted curves in Fig. 10b (classical chain) and Fig. 8h (quantum chain) which have a plateau $-m^z = \frac{1}{6}$). Obviously, as $m^z$ remains constant with varying $\Omega$, the static transverse susceptibility is zero (long–dashed–dotted curves in Fig. 10e). Moreover, $m_n^x$ ($m_n^\perp$), $n = 1, 2, 3$ in this region is zero (Fig. 10h) and the stable ground–state spin configuration is $\theta_n = \theta_{n+1} = \pi$, $\theta_{n+2} = 0$ (see Fig. 11). The Ising magnetization $m^x$ decays as the system runs out the Ising phase according to the power–law, $m^x \sim |\Omega^\star - \Omega|^\beta$, with $\beta = \frac{1}{2}$.

### 4.4. Quantum phase transitions

1D spin systems with short–range interactions do not exhibit singularities in their properties at finite temperatures. The reminiscent of peculiarities in their zero–temperature properties may be expected at low temperatures in the vicinity of the quantum phase transition points.

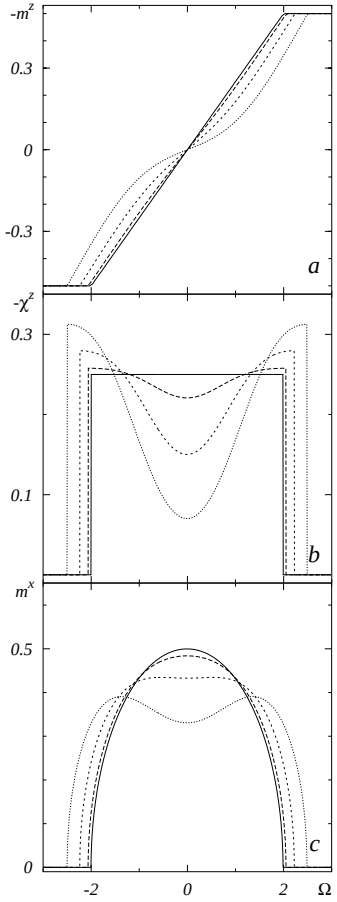


Figure 9. The ground–state transverse magnetization (a), Ising magnetization (c), and static transverse susceptibility (b) curves for the classical transverse Ising/$XX$ chains of period $p = 2$. $I_{1,2} = -1$, $\Omega_{1,2} = \Omega \pm \Delta\Omega$, $\Delta\Omega = 0$ (solid curves), $\Delta\Omega = 0.5$ (long–dashed curves), $\Delta\Omega = 1$ (short–dashed curves), $\Delta\Omega = 1.5$ (dotted curves).



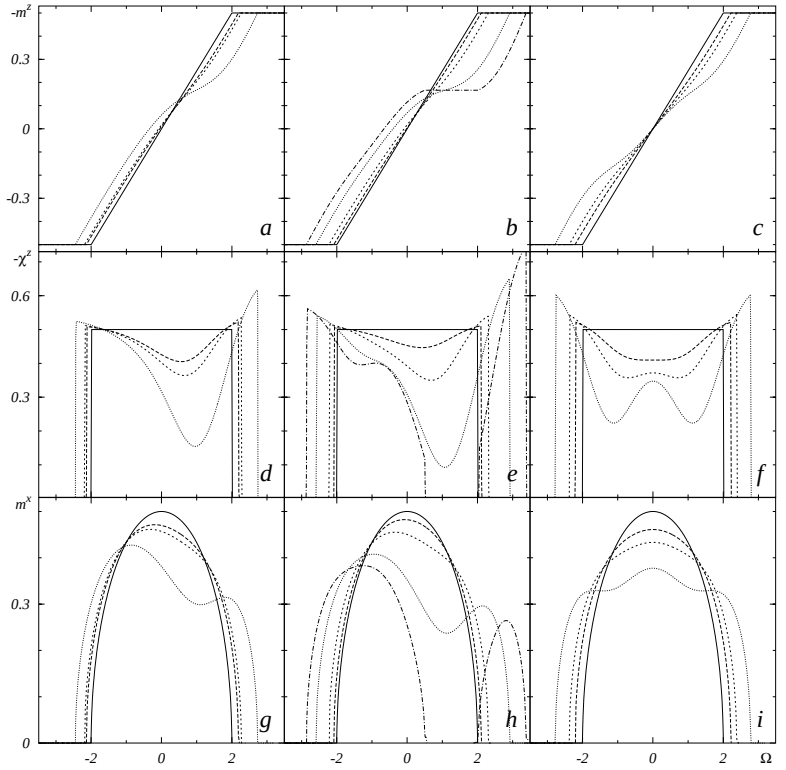


Figure 10. The ground–state transverse magnetization (a, b, c), Ising magnetization (g, h, i), and static transverse susceptibility (d, e, f) curves for the classical transverse Ising/$XX$ chains of period $p = 3$. $I_{1,2,3} = -1$, $\Omega_{1,2,3} = \Omega + \Delta\Omega_{1,2,3}$, $\Delta\Omega_1 + \Delta\Omega_2 + \Delta\Omega_3 = 0$; a, d, g: $\Delta\Omega_2 = \Delta\Omega_1$, $\Delta\Omega_1 = 0$ (solid curves), $\Delta\Omega_1 = 0.5$ (long–dashed curves), $\Delta\Omega_1 = 0.6$ (short–dashed curves), $\Delta\Omega_1 = 1$ (dotted curves); b, e, h: $\Delta\Omega_2 = \frac{1}{2}\Delta\Omega_1$, $\Delta\Omega_1 = 0$ (solid curves), $\Delta\Omega_1 = 0.5$ (long–dashed curves), $\Delta\Omega_1 = 0.85$ (short–dashed curves), $\Delta\Omega_1 = 1.5$ (dotted curves), $\Delta\Omega_1 = 1.9$ (long–dashed–dotted curves); c, f, i: $\Delta\Omega_2 = -\Delta\Omega_1$, $\Delta\Omega_1 = 0$ (solid curves), $\Delta\Omega_1 = 1$ (long–dashed curves), $\Delta\Omega_1 = 1.35$ (short–dashed curves), $\Delta\Omega_1 = 2$ (dotted curves).

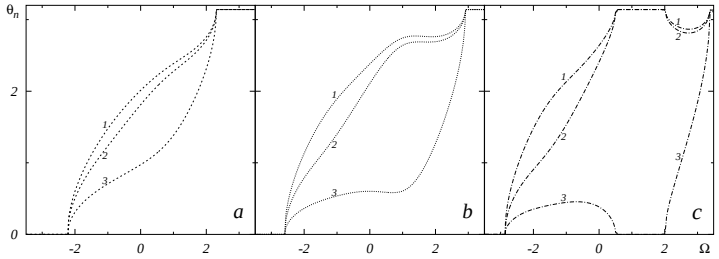


Figure 11. The ground–state spin configuration $\theta_1$, $\theta_2$, $\theta_3$ (the corresponding curves are denoted by 1, 2, 3) for the classical chains of period $p = 3$, $I_{1,2,3} = 1$, $\Omega_{1,2,3} = \Omega + \Delta\Omega_{1,2,3}$, $\Delta\Omega_1 + \Delta\Omega_2 + \Delta\Omega_3 = 0$, $\Delta\Omega_2 = \frac{1}{2}\Delta\Omega_1$, $\Delta\Omega_1 = 0.85$ (a), $\Delta\Omega_1 = 1.5$ (b), $\Delta\Omega_1 = 1.9$ (c) as $\Omega$ varies.

For a regularly alternating transverse Ising chain of period $p$ the quantum phase transition points are determined by Eq. (3.20). The effects of regular alternation on the number and position of the quantum phase transition points in the cases $p = 2$ and $p = 3$ were discussed in Section 3. Although Eq. (3.20) was found many years ago [24] it was not discussed in the context of the quantum phase transition theory. In particular, an important question *how* the gap vanishes as the set of parameters becomes critical was not considered in Ref. [24]. Below we show that two types of critical behaviour are possible: one as it occurs for the second–order phase transition (in Ehrenfest's sense) and another one as it occurs for a weaker singularity (the fourth–order phase transition in Ehrenfest's sense). These findings are confirmed by numerical computations of the two–site spin correlation functions.

First we analyse how the gap vanishes as the set of parameters becomes critical for the case $p = 2$ when $\Omega^\star = \pm\sqrt{\Delta\Omega^2 \pm |I_1 I_2|}$. Eq. (3.16) yields

$$\Delta^2(\Omega) = \Omega^2 + \Delta\Omega^2 + \frac{I_1^2 + I_2^2}{2} - \sqrt{\left(\Omega^2 + \Delta\Omega^2 + \frac{I_1^2 + I_2^2}{2}\right)^2 - \left(\Omega^2 - \Omega^{\star 2}\right)^2} \approx \frac{\left(\Omega^2 - \Omega^{\star 2}\right)^2}{2\left(\Omega^2 + \Delta\Omega^2 + \frac{I_1^2+I_2^2}{2}\right)}. \quad (4.17)$$

If $|\Omega - \Omega^\star| = \epsilon \to 0$ and $\Omega^\star \neq 0$ Eq. (4.17) suggests $\Delta^2(\Omega) \sim \epsilon^2$, i.e., the energy gap vanishes linearly (see Figs. 1, 2). A linear decay of the energy gap can be also seen in many cases in Fig. 3 for chains of period 3. The linearly vanishing gap corresponds to the square–lattice Ising model universality class for critical behaviour. In particular, owing to such a decay of $\Delta$ the ground–state energy per site in the vicinity of $\Omega^\star$ has the form

$$e_0 = -\int_0^\infty \mathrm{d}E E^2 R(E^2) = -\frac{1}{p\pi}\int_{\sqrt{\epsilon^2}}^{\sqrt{a_2}} \mathrm{d}E E^2 \frac{f(E^2)}{\sqrt{E^2 - \epsilon^2}} + \text{analytical with respect to } \epsilon^2 \text{ terms.} \quad (4.18)$$

Here the first term is a contribution of the lowest energy band and the explicit expression for $f(E^2)$ is not important for analysis of nonanalytical behaviour as $\epsilon \to 0$. The first term in (4.18) is proportional to $\epsilon^2 \ln\epsilon$ and as a result the zero–temperature dependence of $m^z$ and $\chi^z$ on $\Omega$ contains the nonanalytical terms $(\Omega - \Omega^\star)\ln|\Omega - \Omega^\star|$ and $\ln|\Omega - \Omega^\star|$, respectively.

Let us turn to the case $p = 2$ with $\Delta\Omega = \sqrt{|I_1 I_2|}$ when we have three critical fields $\Omega^\star = \left\{\pm\sqrt{2|I_1 I_2|}, 0\right\}$ and consider the behaviour of $\Delta(\Omega)$ in the vicinity of $\Omega^\star = 0$, i.e., as $\Omega \to 0$. From Eq. (4.17) one finds that $\Delta^2(\Omega) \sim \epsilon^4$. Repeating the calculation of the ground–state energy (see Eq. (4.18)) for such a decay of $\Delta$ one finds that $e_0$ contains the term $\epsilon^4 \ln\epsilon$ and hence the system exhibits the fourth–order (in Ehrenfest's sense) quantum phase transition at $\Omega^\star = 0$ which is characterized by a logarithmic divergence of the second derivative of the susceptibility $\frac{\partial^2 \chi^z}{\partial \Omega^2}$. (For an example of a fourth–order thermal phase transition see Ref. [29].) For $p = 3$ the dependence $\Delta(\Omega) \sim \epsilon^2$ (see Fig. 3) may occur for the sets of parameters at the boundaries between different regions in Fig. 4 (e.g., at the points b, c, e). Such systems again show the fourth–order quantum phase transition behaviour while approaching the corresponding critical fields.

Our results are in agreement with the scaling relations in the theory of conventional (temperature–driven) phase transitions [30]. Thus, the quantum phase transition in dimension $d = 1$ corresponds to the thermal phase transition in dimension $d+1 = 2$, the exponent $\nu$ which characterizes the divergence of the correlation length $\xi \sim |T - T_c|^{-\nu}$ characterizes the decay of the energy gap $\Delta \sim |\Omega - \Omega^\star|^\nu$, the exponent $\alpha$ characterizing the divergence of the specific heat $c \sim |T - T_c|^{-\alpha}$ characterizes the divergence of the transverse susceptibility $\chi^z \sim |\Omega - \Omega^\star|^{-\alpha}$. Moreover, a number of scaling relations (which do not account for logarithmic di-

vergences) hold. For example, $\alpha = 2 - \nu d$. Substituting $d = 2$, $\nu = 1$ one gets $\alpha = 0$, i.e., only a logarithmic divergence in the dependence $\chi^z$ vs. $\Omega$, whereas for more rapidly decaying energy gap with $\nu = 2$ one finds $\alpha = -2$, i.e., $\chi^z$ does not diverge at $\Omega^\star$ (and only its second derivative exhibits a logarithmic peculiarity).

To discuss further the quantum phases which occur as the transverse field varies we examine the spin correlation functions $\langle s_n^\alpha s_{n+l}^\alpha \rangle$. Unfortunately, we cannot obtain the spin correlation functions of a regularly alternating transverse Ising chain using the continued fraction approach which is restricted to the quantities that can be expressed through the density of states (3.7). However, the spin correlation functions can be determined numerically (see, for example, [31]) for rather long chains of several thousand sites. Knowing $\langle s_n^\alpha s_{n+l}^\alpha \rangle$ we can obtain the on-site magnetization $m_n^{\alpha\,2} = \lim_{r\to\infty} \langle s_n^\alpha s_{n+rp}^\alpha \rangle$. Assuming that $\langle s_n^\alpha s_{n+rp}^\alpha \rangle - \langle s_n^\alpha \rangle \langle s_{n+rp}^\alpha \rangle$ decays as $(rp)^{-\gamma^\alpha} \exp\left(-\frac{rp}{\xi^\alpha}\right)$ if $r \to \infty$ we can also find the correlation length $\xi^\alpha$ and the power–law exponent $\gamma^\alpha$. In our calculations we consider chains with $N = 2000$ ($p = 2$) or $N = 2100$ ($p = 3$), we take $n = 500$, $rp = 1000$ ($p = 2$) or $rp = 999$ ($p = 3$) to determine $|m_j^x|$ and $rp = 40$ ($p = 2$) or $rp = 60, \ldots, 360$ ($p = 3$) to determine $\xi^x$ and $\gamma^x$. Our findings are collected in Figs. 12, 13.

As can be seen from these figures the behaviour of the Ising magnetization $m^x$ (which plays the role of the order parameter) indicates the different phases (Ising phase if $m^x \neq 0$ or paramagnetic phase if $m^x = 0$) and the phase transitions between them. For a set of parameters which yields weak singularities (i.e., $m^x = 0$ in the Ising phase, see Figs. 12b, 13b, 13c, 13e) the finite–size effects are strong and the finite–chain result for $x$–magnetization tends to zero very slowly with increasing $N$. For the second–order quantum phase transition points the critical behaviour is given by $m^x \sim |\Omega^\star - \Omega|^\beta$ with $\beta = \frac{1}{8}$. The appearance/disappearance of the Ising magnetization is accompanied by a divergence of the correlation length $\xi^x = |\Omega - \Omega^\star|^{-\nu}$ with $\nu = 1$ for the second–order quantum phase transition points and with $\nu = 2$ for the fourth–order quantum phase transition points (Figs. 12d – 12f, Figs. 13g – 13l) that is in agreement with the values of exponent characterizing the energy gap behaviour. At $\Omega = \Omega^\star$ the $xx$ spin correlation functions show power–law decay with the exponent $\gamma^x = \frac{1}{4}$ (Figs. 12g – 12i, Figs. 13m – 13r). Finally, the results for spin correlation functions at special values of the transverse field $\Omega$ (when one on–site field equals zero) coincide with the analytical predictions obtained above using the cluster Hamiltonian eigenvectors (see (4.5), (4.6)). For example, for the chain



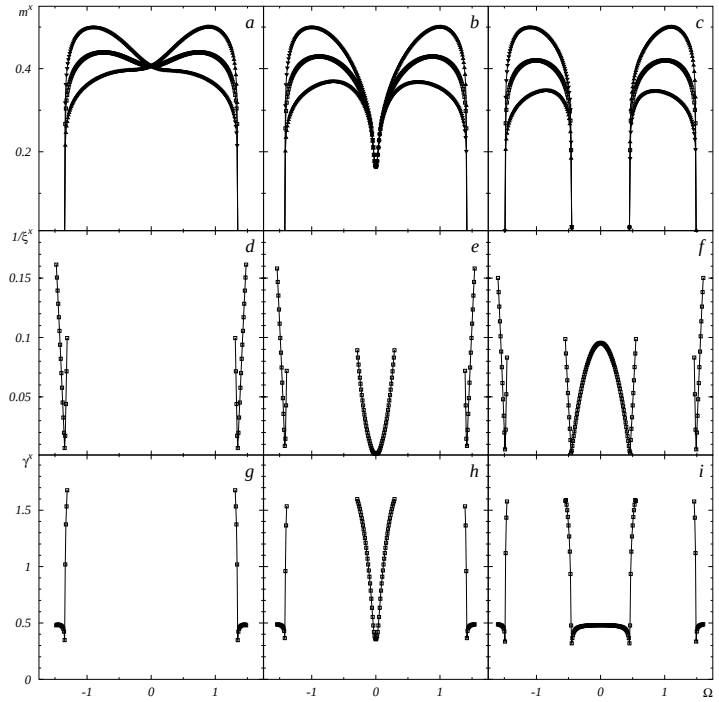


Figure 12. The ground–state sublattice $x$–magnetizations $|m_j^x|$, $j = 1, 2$ (triangles) and $m^x = \frac{1}{2}(|m_1^x| + |m_2^x|)$ (squares) (a, b, c), inverse correlation length $\frac{1}{\xi^x}$ (d, e, f), and $\gamma^x$ (g, h, i) for the transverse Ising chain of period 2 with $|I_1| = |I_2| = 1$, $\Omega_{1,2} = \Omega \pm \Delta\Omega$, $\Delta\Omega = 0.9$ (a, d, g), $\Delta\Omega = 1$ (b, e, h), $\Delta\Omega = 1.1$ (c, f, i). Connecting curves are guides to the eye.

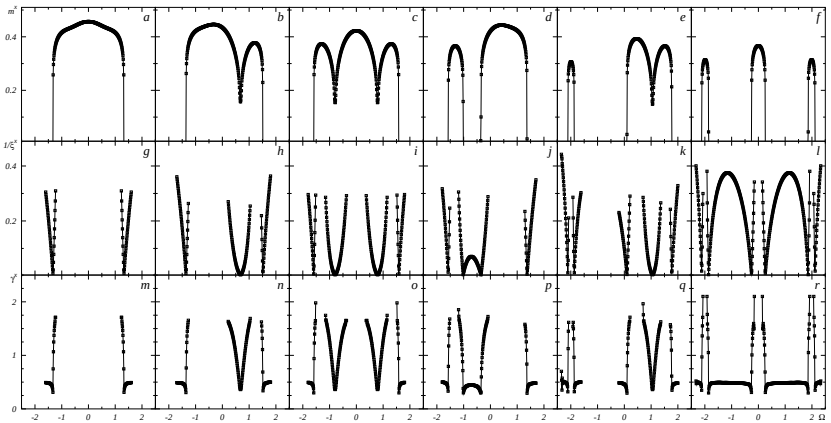

Figure 13. The ground–state $x$–magnetization $m^x = \frac{1}{3}\left(|m_1^x| + |m_2^x| + |m_3^x|\right)$ (a, b, c, d, e, f), inverse correlation length $\frac{1}{\xi^x}$ (g, h, i, j, k, l), and $\gamma^x$ (m, n, o, p, q, r) for the transverse Ising chain of period 3 with $|I_1| = |I_2| = |I_3| = 1$, $\Omega_{1,2,3} = \Omega + \Delta\Omega_{1,2,3}$, $\Delta\Omega_1 + \Delta\Omega_2 + \Delta\Omega_3 = 0$, $\Delta\Omega_1 = 1$, $\Delta\Omega_2 = 0$ ($\Omega^\star \approx \{\pm 1.325\}$) (a, g, m), $\Delta\Omega_1 = 1$, $\Delta\Omega_2 \approx 0.292$ ($\Omega^\star \approx \{-1.355, 0.678, 1.513\}$) (b, h, n), $\Delta\Omega_1 = \left(\frac{27}{4}\right)^{\frac{1}{6}} \approx 1.374$, $\Delta\Omega_2 = 0$ ($\Omega^\star \approx \{\pm 0.794, \pm 1.587\}$) (c, i, o), $\Delta\Omega_1 = \left(\frac{27}{4}\right)^{\frac{1}{6}} \approx 1.374$, $\Delta\Omega_2 = -1$ ($\Omega^\star \approx \{-1.574, -1.020, -0.348, 1.367\}$) (d, j, p), $\Delta\Omega_1 = 2$, $\Delta\Omega_2 \approx -1.575$ ($\Omega^\star \approx \{-2.107, -1.874, 0.102, 1.054, 1.772\}$) (e, k, q), $\Delta\Omega_1 = 2$, $\Delta\Omega_2 = 0$ ($\Omega^\star \approx \{\pm 0.254, \pm 1.861, \pm 2.115\}$) (f, l, r). Connecting curves are guides to the eye. The taken sets of parameters are in correspondence with the points a, b, c, d, e, f in Fig. 4.



of period 3 with $I_1 = I_2 = I_3 = 1$, $\Delta\Omega_1 = 1$, $\Delta\Omega_2 = 0$, $\Delta\Omega_3 = -1$ at $\Omega = -1$

$$|m_1^x| = \frac{1}{2}, \quad |m_2^x| \approx 0.417, \quad |m_3^x| \approx 0.331$$

(see Fig. 13a) whereas for such a chain with $\Delta\Omega_1 = 2$, $\Delta\Omega_2 = 0$, $\Delta\Omega_3 = -2$ at $\Omega = -2$

$$|m_1^x| = \frac{1}{2}, \quad |m_2^x| \approx 0.267, \quad |m_3^x| \approx 0.175$$

(see Fig. 13f). It should be noted that the Ising magnetization at the sites with zero transverse fields has its maximal value $\frac{1}{2}$. Probably the most spectacular feature of the Ising chain with regularly alternating transverse field is the reentrant behaviour with varying $\Omega$ nicely seen in Figs. 12c, 13d – 13f. The appearance of the paramagnetic phase at intermediate values of the transverse field when $x$–magnetization is zero and $z$–magnetization is almost constant can be associated with the following classical picture. Assume, for example, $p = 2$ and $\Omega = 0$; then owing to the regularly varying on–site transverse fields $\pm\Delta\Omega$ with large $\Delta\Omega$ all on–site magnetizations are directed in $\pm z$–direction in the spin space. Naturally, this picture may play only an auxiliary role for the considered quantum systems.

## 5. Temperature behaviour of the specific heat

We turn to a discussion of the effects of regular alternation on the temperature dependence of the specific heat (3.13). The low–temperature behaviour of this quantity is determined by the fact whether the system is gapped or gapless. Thus, the zero–energy excitations according to (3.13) immediately produce a linear dependence of the specific heat on temperature. As a result the low–temperature behaviour of the specific heat indicates the quantum phase transition points that can be seen in Figs. 14, 15 in complete agreement with the outcomes which follow from the behaviour of the $xx$ spin correlation functions shown in Figs. 12, 13.

Moreover, the regular alternation may produce many–peak structure of the temperature profiles of the specific heat. We may easy clarify the dependence $c$ vs. $T$ for different fields $\Omega$ for the case $p = 2$ when $\Omega_{1,2} = \Omega$ and $I_{1,2} = I(1 \pm \delta)$ in the strong coupling limit $\delta = 1$. The eigenvalues of the 2–site cluster Hamiltonian are $\pm\sqrt{\Omega^2 + \frac{I^2}{4}}$, $\pm\frac{I}{2}$ (see the first column

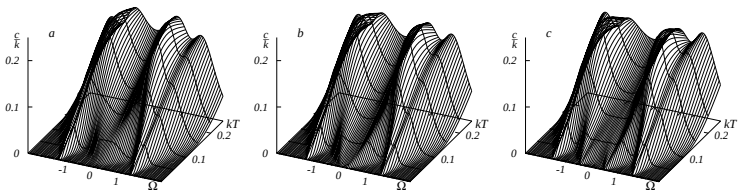


Figure 14. The low–temperature behaviour of the specific heat for the transverse Ising chain of period 2 with $|I_1| = |I_2| = 1$, $\Omega_{1,2} = \Omega \pm \Delta\Omega$, $\Delta\Omega = 0.9$ (a), $\Delta\Omega = 1$ (b), $\Delta\Omega = 1.1$ (c).

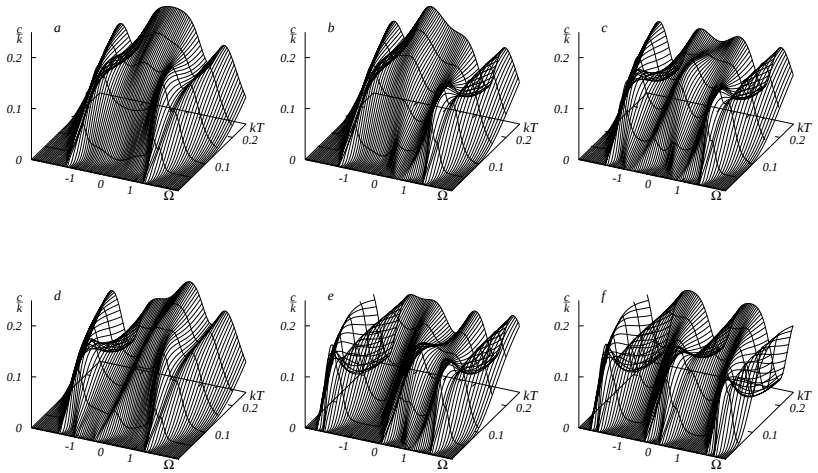


Figure 15. The low–temperature behaviour of the specific heat for the transverse Ising chain of period 3 with $|I_1| = |I_2| = |I_3| = 1$, $\Omega_{1,2,3} = \Omega + \Delta\Omega_{1,2,3}$, $\Delta\Omega_1 + \Delta\Omega_2 + \Delta\Omega_3 = 0$, $\Delta\Omega_1 = 1$, $\Delta\Omega_2 = 0$ (a), $\Delta\Omega_1 = 1$, $\Delta\Omega_2 \approx 0.292$ (b), $\Delta\Omega_1 \approx 1.374$, $\Delta\Omega_2 = 0$ (c), $\Delta\Omega_1 \approx 1.374$, $\Delta\Omega_2 = -1$ (d), $\Delta\Omega_1 = 2$, $\Delta\Omega_2 \approx -1.575$ (e), $\Delta\Omega_1 = 2$, $\Delta\Omega_2 = 0$ (f).



in Table 4.1). Therefore, the Helmholtz free energy per site is

$$
\begin{aligned}
f &= -\frac{1}{2\beta}\ln\left(2\cosh\left(\beta\sqrt{\Omega^2+\frac{I^2}{4}}\right)+2\cosh\left(\frac{\beta I}{2}\right)\right)\\
&= -\frac{2}{\beta}\int_0^\infty \mathrm{d}E E R(E^2)\ln\left(2\cosh\frac{\beta E}{2}\right),\\
R(E^2) &= \frac{1}{2}\left(\delta\left(E^2-\left(\sqrt{\Omega^2+\frac{I^2}{4}}-\frac{I}{2}\right)^2\right)\right.\\
&\quad\left.+\delta\left(E^2-\left(\sqrt{\Omega^2+\frac{I^2}{4}}+\frac{I}{2}\right)^2\right)\right). \qquad (5.1)
\end{aligned}
$$

Analyzing now the integrand in the formula for the specific heat (3.13) with $R(E^2)$ (5.1) one concludes that for small $\Omega$ the temperature profile of the specific heat should have two–peak structure whereas for large $\Omega$ the two–peak structure should disappear. This conclusion remains valid if $R(E^2)$ corresponds to two subbands with finite widths.

## 6. Anisotropic $XY$ chain without field

### 6.1. The density of states

As a byproduct of the study of regularly alternating transverse Ising chains we obtain the thermodynamic quantities of regularly alternating anisotropic $XY$ chains without field (2.4). Really, using the unitary transformations discussed in the end of Section 2 we can state that the Helmholtz free energy of the regularly alternating anisotropic $XY$ chain without field (2.4) defined by a sequence of parameters $I_1^x I_1^y I_2^x I_2^y \ldots I_p^x I_p^y I_1^x I_1^y I_2^x I_2^y \ldots I_p^x I_p^y \ldots$ is given by Eq. (3.8) with $R(E^2)$ (3.10) and the diagonal Green functions involved into Eq. (3.10) are

determined as follows

$$G_{nn} = \frac{1}{E^2 - {I^x_{n-1}}^2 - {I^y_n}^2 - \Delta^-_n - \Delta^+_n}, \tag{6.1}$$

$$\Delta^-_n = \cfrac{{I^y_{n-2}}^2 {I^x_{n-1}}^2}{E^2 - {I^x_{n-3}}^2 - {I^y_{n-2}}^2 - \cfrac{{I^y_{n-4}}^2 {I^x_{n-3}}^2}{E^2 - {I^x_{n-5}}^2 - {I^y_{n-4}}^2 - \ddots}},$$

$$\Delta^+_n = \cfrac{{I^y_n}^2 {I^x_{n+1}}^2}{E^2 - {I^x_{n+1}}^2 - {I^y_{n+2}}^2 - \cfrac{{I^y_{n+2}}^2 {I^x_{n+3}}^2}{E^2 - {I^x_{n+3}}^2 - {I^y_{n+4}}^2 - \ddots}}.$$

Moreover, we may use the obtained densities of states (3.16), (3.17) to find the thermodynamic quantities of some regularly alternating anisotropic $XY$ chains. Thus, the anisotropic $XY$ chain of period 2 is unitary equivalent to two different transverse Ising chains both of period 1 and as a result

$$R(E^2) = \begin{cases} \frac{1}{2\pi}\frac{1}{\sqrt{\mathcal{A}_{xy}(E^2)}}, & \text{if} \quad \mathcal{A}_{xy}(E^2) > 0 \\ 0, & \text{otherwise} \end{cases} + \begin{cases} \frac{1}{2\pi}\frac{1}{\sqrt{\mathcal{A}_{yx}(E^2)}}, & \text{if} \quad \mathcal{A}_{yx}(E^2) > 0, \\ 0, & \text{otherwise}, \end{cases} \tag{6.2}$$

$$\mathcal{A}_{\alpha\beta}(E^2) = -\left(E^2 - \left(I^\alpha_1 - I^\beta_2\right)^2\right)\left(E^2 - \left(I^\alpha_1 + I^\beta_2\right)^2\right).$$

(Note, that for the isotropic case $I^x_1 = I^y_1 = I_1$, $I^x_2 = I^y_2 = I_2$, Eq. (6.2) yields the result obtained in Ref. [23] (Eqs. (9) – (11) of that paper); in the anisotropic case Eq. (6.2) agrees with (3.18).) The anisotropic $XY$ chain of period 3 after performing the above mentioned unitary transformations is equivalent to two identical transverse Ising chains of period 3 and therefore $R(E^2)$ is given by Eq. (3.17) after the substitution $\Omega_1 \to I^y_1$, $I_1 \to I^x_2$, $\Omega_2 \to I^y_3$, $I_2 \to I^x_1$, $\Omega_3 \to I^y_2$, $I_3 \to I^x_3$. Let us also note, that the anisotropic $XY$ chains of period 4 (6) are unitary equivalent to two different transverse Ising chains of period 2 (3) and hence Eq. (3.16) (Eq. (3.17)) after simple substitutions yield the thermodynamic properties of such chains.



### 6.2. The influence of the exchange interaction anisotropy on spin–Peierls dimerization

Let us use the ground–state energy per site

$$e_0 = -2\int_0^\infty \mathrm{d}E E^2 R(E^2) \tag{6.3}$$

of the anisotropic $XY$ chain of period 2 to examine the effects of the exchange interaction anisotropy on the spin–Peierls dimerization inherent in the isotropic $XY$ chain [32, 33]. For this purpose we assume in (6.2), (6.3) $I^x_1 = (1+\delta)(1+\gamma)$, $I^y_1 = (1+\delta)(1-\gamma)$, $I^x_2 = (1-\delta)(1+\gamma)$, $I^y_2 = (1-\delta)(1-\gamma)$ where $0 \le \delta < 1$ is the dimerization parameter and $0 \le \gamma \le 1$ is the exchange interaction anisotropy parameter. We consider the total energy per site $\mathcal{E}(\delta)$ and its dependence on $\delta$. $\mathcal{E}(\delta)$ consists of the magnetic part $e_0(\delta)$ (6.3) and the elastic part $\alpha\delta^2$. Let us recall that in the isotropic limit $\gamma = 0$ the total energy $\mathcal{E}(\delta)$ exhibits a minimum at a nonzero value of the dimerization parameter $\delta^\star \neq 0$ that is a manifestation of lattice instability with respect to spin–Peierls dimerization [32]. In the other limiting case $\gamma = 1$ the magnetic energy does not depend on $\delta$ and hence the uniform lattice is stable. In Fig. 16a one can see how the behaviour of $\mathcal{E}(\delta)$ vs. $\delta$ varies as $\gamma$ increases from 0 to 0.4 for $\alpha = 0.5$. At $\gamma = 0$ the total energy $\mathcal{E}(\delta)$ exhibits a minimum at a nonzero value of dimerization parameter $\delta^\star \neq 0$. As $\gamma$ increases the dependence remains qualitatively the same with, however, slightly decreasing value of $\delta^\star$ (see Figs. 16b and 16c). At certain value of anisotropy parameter $\gamma_A$ an additional minimum at $\delta = 0$ appears, both minimum are separated by a maximum, the minimum at $\delta^\star \neq 0$ remains the deeper one. At the value of $\gamma_B$ ($> \gamma_A$) the minima have the same depth and with further increase of $\gamma$ the minimum at $\delta = 0$ becomes the deeper one. If $\gamma$ exceeds $\gamma_C$ ($> \gamma_B$) the minimum for a nonzero dimerization parameter disappears. In Fig. 16b one can see the behaviour of $\delta^\star$ as $\gamma$ varies from 0 to 0.4 for different $\alpha$s (solid curves; the dashed curves show the behaviour of the maximum in the dependence $\mathcal{E}(\delta)$ vs. $\delta$); in Fig 16c one can see the dependence of $\delta^\star$ on $\gamma$ for $\alpha = 0.4,\ 0.5,\ 0.6$. The bold dots in the curves in this panel correspond to the characteristic values of the anisotropy parameter $\gamma_A < \gamma_B < \gamma_C$ discussed above. The influence of the anisotropy on the spin–Peierls dimerized phase occurs according to the first–order phase transition scenario. The corresponding phase diagram is shown in Fig. 16d where we indicate the region of stability of the dimerized (A) and uniform (C) phases as well as the metastable region (regions $B_1$ and $B_2$) where both phases may coexist.

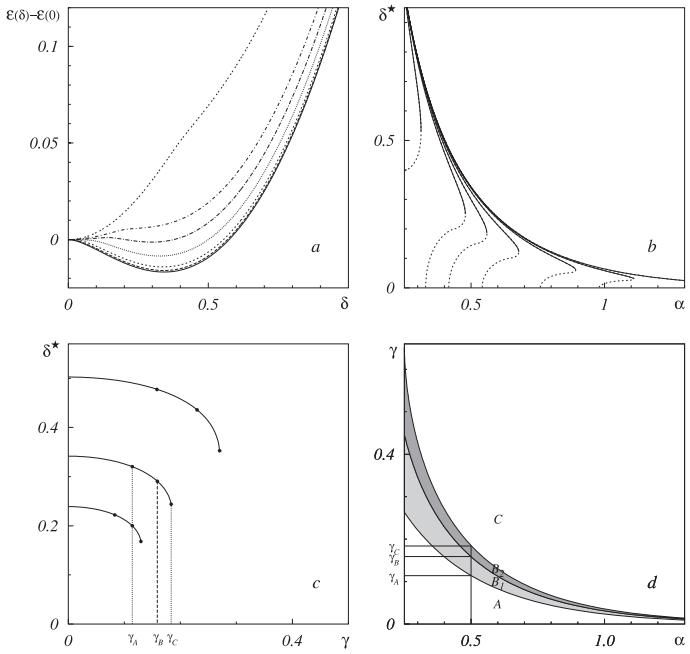


Figure 16. The total ground–state energy per site $\mathcal{E}(\delta)$ vs. dimerization parameter $\delta$ ($\alpha = 0.5$, from bottom to top $\gamma = 0$, 0.025, 0.05, 0.1, 0.15, 0.2, 0.4) (a), the dimerization parameter $\delta^\star$ vs. $\alpha$ (from right to left $\gamma = 0$, 0.025, 0.05, 0.1, 0.15, 0.2, 0.4) (b), the dimerization parameter $\delta^\star$ vs. $\gamma$ (from top to bottom $\alpha = 0.4$, 0.5, 0.6; the meaning of the characteristic values of the anisotropy parameter $\gamma_A$, $\gamma_B$, $\gamma_C$ (denoted for $\alpha = 0.5$) is explained in the main text) (c), and the phase diagram in the plane $\alpha - \gamma$ (in the region A (C) the dimerized (uniform) phase occurs; in the regions $B_1$, $B_2$ both phases are possible although in the region $B_1$ ($B_2$) the dimerized (uniform) phase is favourable) (d).



It is interesting to compare the described effects of the exchange interaction anisotropy on the spin–Peierls dimerized phase with the effects of the transverse field on the spin–Peierls dimerized phase [23, 33]. Similarly to the anisotropy $\gamma$ the transverse field $\Omega$ destroys the dimerized phase according to a first–order phase transition scenario. However, the value of the dimerization parameter $\delta^\star$ remains unchanged as $\Omega$ increases until $\Omega_C$.

## 7. Concluding remarks

In this work we have analyzed in some detail the ground–state and thermodynamic properties of regularly alternating spin–$\frac{1}{2}$ transverse Ising chains and anisotropic $XY$ chains without field. Due to the Jordan–Wigner mapping and the continued fraction approach we can calculate the thermodynamic quantities rigorously analytically. Moreover, for certain values of parameters we can also calculate the ground–state spin correlation functions. For other values of parameters we have calculated the spin correlation functions numerically for long chains consisting of few thousand sites. We have shown how the ground–state properties of regularly alternating classical transverse Ising/$XX$ chains can be examined. The main new results obtained are as follows. First, we have examined the effects of regular alternation on quantum phases and quantum phase transitions in the transverse Ising chain. Owing to regularly alternating parameters the number of quantum phase transition may increase (but never exceeds $2p$ where $p$ is the period of alternation), the critical behaviour remains as in the uniform chain, however, a weaker singularity may appear. Second, we have demonstrated how the plateaus in the ground–state magnetization curves for the classical regularly alternating transverse Ising/$XX$ chains may emerge. Third, we have shown how the exchange interaction anisotropy destroys the spin–Peierls dimerization inherent in the spin–$\frac{1}{2}$ isotropic $XY$ chain. The performed study provides a set of reference results which may be useful for understanding more complicated quantum spin chains.

## Acknowledgments

The present study was partly supported by the DFG over a few past years a number of times (projects 436 UKR 17/7/01, 436 UKR 17/1/02, 436 UKR 17/17/03). O. D. acknowledges the kind hospitality of the Magdeburg University in the autumn of 2003 when the paper was completed. The paper was partly presented at the 19th General Conference of the

EPS Condensed Matter Division held jointly with CMMP 2002 – Condensed Matter and Materials Physics (Brighton, UK, 2002), at the 28th Conference of the Middle European Cooperation in Statistical Physics (Saarbrücken, Germany, 2003) and at the International Workshop and Seminar on Quantum Phase Transitions (Dresden, Germany, 2003). O. D. expresses appreciation to the Institute of Physics for the support for participation. O. D. and O. Z. thank the organisers of the MECO conference for the support. O. D. is grateful to the Max–Planck–Institut für Physik komplexer Systeme for the hospitality in Dresden.

## References

1. E. Lieb, T. Schultz, and D. Mattis, Ann. Phys. (N.Y.) **16,** 407 (1961).
2. E. Fradkin, Field Theories of Condensed Matter Systems (Addison–Wesley Publishing Company: Redwood City, California Menlo Park, California Reading, Massachusetts New York Don Mills, Ontario Workingham, United Kingdom Amsterdam Bonn Sydney Singapore Tokyo Madrid San Juan, 1991).
3. B. K. Chakrabarti, A. Dutta, and P. Sen, Quantum Ising Phases and Transitions in Transverse Ising Models (Springer–Verlag: Berlin Heidelberg, 1996).
4. S. Sachdev, Quantum Phase Transitions (Cambridge University Press: Cambridge New York Melbourne Madrid, 1999).
5. P. Pfeuty, Ann. Phys. (N.Y.) **57,** 79 (1970).
6. J. M. Luck, J. Stat. Phys. **72,** 417 (1993).
7. D. S. Fisher, Phys. Rev. Lett. **69,** 534 (1992);
   D. S. Fisher, Phys. Rev. B **51,** 6411 (1995).
8. F. Iglói, L. Turban, D. Karevski, and F. Szalma, Phys. Rev. B **56,** 11031 (1997).
9. Jong–Won Lieh, J. Math. Phys. **11,** 2114 (1970).
10. J. H. H. Perk, H. W. Capel, M. J. Zuilhof, and Th. J. Siskens, Physica A **81,** 319 (1975).
11. K. Okamoto and K. Yasumura, J. Phys. Soc. Jap. **59,** 993 (1990).
12. L. L. Gonçalves and J. P. de Lima, J. Phys.: Condens. Matter **9,** 3447 (1997).
13. F. F. B. Filho, J. P. de Lima, and L. L. Gonçalves, J. Magn. Magn. Mater. **226–230,** 638 (2001).
14. P. Tong and M. Zhong, Physica B **304,** 91 (2001).
15. F. Ye, G. – H. Ding, and B. – W. Xu, cond-mat/0105584.
16. M. Arlego, D. C. Cabra, J. E. Drut, and M. D. Grynberg, Phys. Rev. B **67,** 144426 (2003).



17. O. Derzhko, J. Phys. A **33,** 8627 (2000);
    O. Derzhko, Czechoslovak Journal of Physics **52,** A277 (2002).
18. D. C. Mattis, The Theory of Magnetism II. Thermodynamics and Statistical Mechanics (Springer–Verlag: Berlin Heidelberg New York Tokyo, 1985).
19. H. Braeter and J. M. Kowalski, Physica A **87,** 243 (1977).
20. P. Henelius and S. M. Girvin, Phys. Rev. B **57,** 11457 (1998).
21. O. V. Derzhko and T. Ye. Krokhmalskii, Visn. L'viv. Univ., Ser. Fiz. (L'viv) 26, 47 (1993) (in Ukrainian);
    O. Derzhko and T. Krokhmalskii, Ferroelectrics **153,** 55 (1994).
22. J. Slechta, J. Phys. C **10,** 2047 (1977).
23. O. Derzhko, J. Richter, and O. Zaburannyi, Physica A **282,** 495 (2000).
24. P. Pfeuty, Phys. Lett. A **72,** 245 (1979).
25. O. Derzhko, Ukrainian Journal of Physics **46,** 762 (2001).
26. O. Derzhko, J. Richter, T. Krokhmalskii, and O. Zaburannyi, Phys. Rev. B **66,** 144401 (2002);
    O. Derzhko, J. Richter, T. Krokhmalskii, and O. Zaburannyi, Acta Physica Polonica B **34,** 1387 (2003).
27. J. P. de Lima and L. L. Gonçalves, J. Magn. Magn. Mater. **206,** 135 (1999).
28. G. S. Joyce, Phys. Rev. **155,** 478 (1967).
29. P. Kumar, D. Hall, and R. G. Goodrich, Phys. Rev. Lett. **82,** 4532 (1999);
    P. Kumar, cond-mat/0207373.
30. S. – K. Ma, Modern Theory of Critical Phenomena (Addison-Wesley Publishing: Reading, Mass., London, Benjamin, 1976).
31. O. Derzhko and T. Krokhmalskii, Phys. Rev. B **56,** 11659 (1997);
    O. Derzhko and T. Krokhmalskii, physica status solidi (b) **208,** 221 (1998).
32. P. Pincus, Solid State Commun. **9,** 1971 (1971).
33. J. H. Taylor and G. Müller, Physica A **130,** 1 (1985).

Препринти Інституту фізики конденсованих систем НАН України розповсюджуються серед наукових та інформаційних установ. Вони також доступні по електронній комп'ютерній мережі на WWW-сервері інституту за адресою http://www.icmp.lviv.ua/

The preprints of the Institute for Condensed Matter Physics of the National Academy of Sciences of Ukraine are distributed to scientific and informational institutions. They also are available by computer network from Institute's WWW server (http://www.icmp.lviv.ua/)

Олег Володимирович Держко
Йоганес Ріхтер
Тарас Євстахійович Крохмальський
Олесь Володимирович Забуранний

Властивості в основному стані і термодинамічні властивості регулярнозмінних спін–$\frac{1}{2}$ анізотропних $XY$ ланцюжків

Роботу отримано 25 березня 2005 р.

Затверджено до друку Вченою радою ІФКС НАН України

Рекомендовано до друку семінаром відділу теорії модельних спінових систем

Виготовлено при ІФКС НАН України